Basin Research (1997) **9,** 275–302

Regular spacing of drainage outlets from linear fault blocks

Peter J. Talling,* Michael D. Stewart,† Colin P. Stark,‡ Sanjeev Gupta‡ and Stephen J. Vincent§

**Department of Geology, Bristol University, Bristol BS8 1RJ, UK*
†Department of Geography, Bristol University, Bristol BS8 1SS, UK
‡Department of Earth Sciences, Oxford University, Oxford OX1 3PR, UK
§Cambridge Arctic Shelf Programme, Cambridge CB2 3EQ, UK

ABSTRACT

Outlets of river basins located on fault blocks often show a regular spacing. This regularity is most pronounced for fault blocks with linear ridge crests and a constant half-width, measured perpendicular to the ridge crest. The ratio of the half-width of the fault block and the outlet spacing is used in this study to characterize the average shape (or spacing ratio) of 31 sets of drainage basins. These fault-block spacing ratios are compared with similar data from small-scale flume experiments and large-scale mountain belts. Fault-block spacing ratios are much more variable than those measured for mountain belts. Differences between fault-block spacing ratios are attributed to variability in factors influencing the initial spacing of channel heads and subsequent rates of channel incision during the early stages of channel network growth (e.g. initial slope and uplift rate, precipitation, runoff efficiency and substrate erodibility). Widening or narrowing of fault blocks during ongoing faulting will also make spacing ratios more variable. It is enigmatic that some of these factors do not produce similar variability in mountain belt spacing ratios. Flume experiments in which drainage networks were grown on static topography show a strong correlation between spacing ratios and surface gradient. Spacing ratios on fault blocks are unaffected by variations in present-day gradients. Drainage basins on the Wheeler Ridge anticline in central California, which have formed on surfaces progressively uplifted by thrust faulting during the last 14 kyr, demonstrate that outlet spacing is likely to be determined during the early stages of drainage growth. This dependency on initial conditions may explain the lack of correlation between spacing ratios of fault blocks and slopes measured at the present day.

Spacing ratios determine the location of sediment supply points to adjacent areas of deposition, and hence strongly influence the spatial scale of lateral facies variations in the proximal parts of sedimentary basins. Spacing ratios may be used to estimate this length scale in ancient sedimentary basins if the width of adjacent topography is known. Spacing ratio variability makes these estimates much less precise for fault blocks than for mountain belts.

INTRODUCTION

Simple observation of topographic maps indicates that the spacing of drainage basin outlets is often remarkably consistent along the same mountain front (Wallace, 1978; Adams, 1985; Mayer, 1986; Talling *et al.*, 1992, 1993). This regularity in outlet spacing is particularly marked for fault blocks with straight mountain fronts and ridge crests. The relatively uniform width of such fault blocks, together with the regularity in outlet spacing, results in a characteristic drainage basin shape and area (Fig. 1A).

Regularity in drainage basin shape and outlet spacing has significant implications for patterns of deposition in adjacent sedimentary basins, and hence for the geometry of their sedimentary fills. Drainage basin outlets represent the points at which sediment is supplied to the basin. The spacing of alluvial fans or fan deltas in a direction parallel to the mountain front is determined by the outlet spacing (Figs 1B and 2). Patterns of deposition are also affected by rates of sediment supply to the drainage outlets. Drainage basin shape, which determines drainage basin area, is a fundamental control on these supply rates

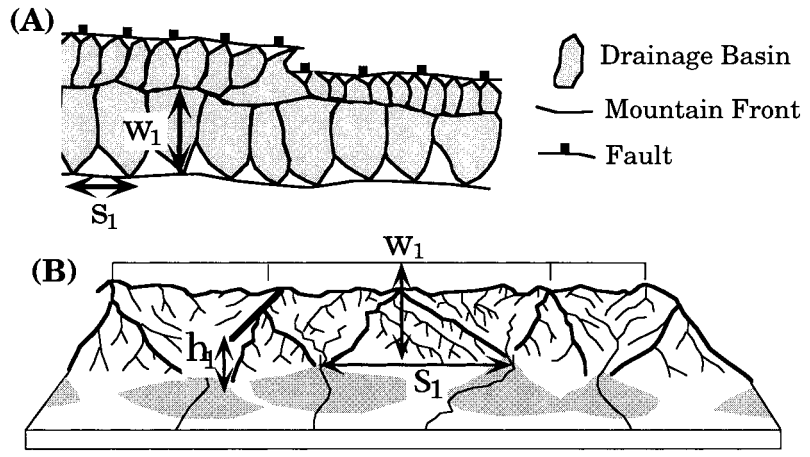

Fig. 1. (A) Schematic map view of drainage basins on a linear fault block. (B) Schematic perspective view of a linear fault block showing the parameters measured in this study (after Hovius, 1996). The topographic half width (w) was measured from the mountain front to drainage divide, in a direction perpendicular to the mountain front. The outlet spacing (s) was measured in a straight line between adjacent drainage outlets. The topographic relief (h) was measured as the elevation difference between the mountain front and drainage divide.

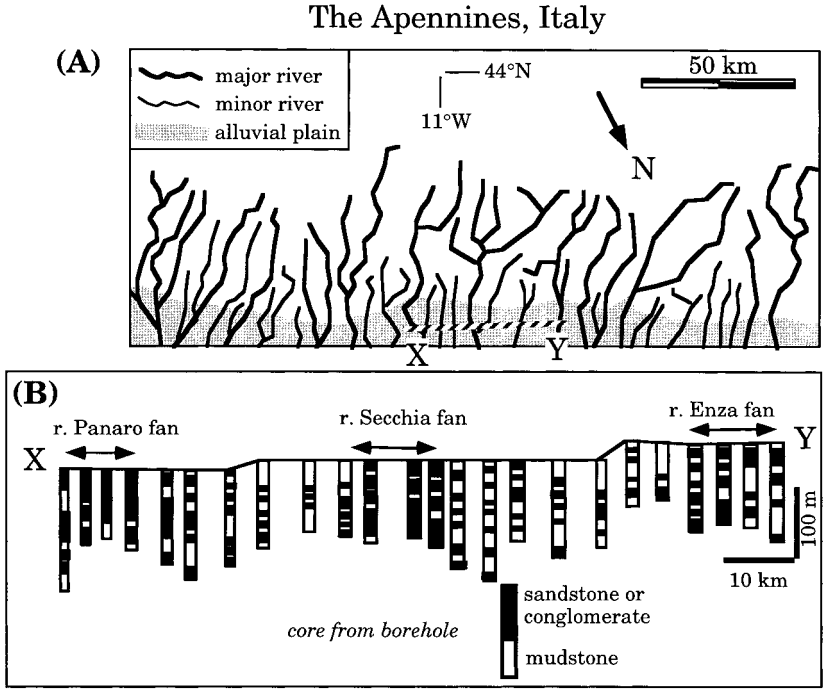

Fig. 2. (A) Map view of the drainage pattern of the Northern Apennines in Italy. (B) Vertical section through the basin-fill in the adjacent sedimentary basin. The relative abundance of coarse and fine alluvial deposits in boreholes is indicated. Note that the abundance of coarse deposits increases near the drainage outlet of the rivers Enza, Secchia and Panaro (after Ori, 1993).

(Milliman & Syvitski, 1992). The importance of drainage basin area for depositional patterns is illustrated by the correlation between alluvial fan size and drainage basin area that has been well documented in a number of locations (e.g. Bull, 1964; Hooke & Rohrer, 1979; Kostaschuk *et al.*, 1986). Regularity in both outlet spacing and drainage basin area will result in regularly spaced facies changes in the basin fill (Fig. 2). As facies changes affect patterns of fluid flow in the subsurface, predicting the length scales of these changes has important implications for developing hydrocarbon reservoirs (e.g. Flint & Bryant, 1993) or modelling groundwater flow. Previous work has shown how relatively large drainage basins are commonly associated with the boundaries of extensional fault segments (Leeder & Gawthorpe, 1987). The large alluvial fans associated with such drainage basins are favourable sites for hydrocarbon reservoirs in rift basins (Leeder & Gawthorpe, 1987).

Hovius (1996) has quantitatively documented the degree of regularity in drainage outlet spacing in modern, large-scale compressional orogens with linear trends. The ratio of mountain belt width to mean outlet spacing (spacing ratio, R) was found to be strikingly uniform for such orogens (Hovius, 1996). For 11 orogens, the spacing ratio only varied between 1.91 and 2.23. Hovius (1996) illustrated how this uniform spacing ratio can be used, together with field evidence constraining the location of alluvial fan apices, to determine the width of ancient compressional orogens. The initial aim of the present study is to quantitatively document whether drainage outlets are regularly spaced along topography uplifted by a single fault (uplift in orogens occurs due to multiple faults), and to determine whether these data can be used to predict facies variations in adjacent sedimentary basins.

Drainage basin morphology has the potential to provide important constraints on the rate and spatial migration of uplift in areas of active faulting. At present, such information is not widely utilized in neotectonic studies, a notable exception being recent work linking drainage basin shapes to the spatial evolution of fault segment

boundaries (Jackson & Leeder, 1994; Jackson *et al.*, 1996; Densmore *et al.*, 1997). In order to decipher the information on tectonic processes provided by drainage basin shape and spacing we need to understand the processes by which drainage basins form and grow. The second aim of this paper is to identify these processes and their controlling variables by comparing the spacing and shape of drainage basins observed on fault blocks, with similar data from larger-scale mountain belts (Hovius, 1996), smaller-scale flume experiments (Schumm *et al.*, 1987) and computer simulations of drainage growth (e.g. Howard, 1994). This comparison allows the effects of processes which act over different length scales to be assessed. For instance, river capture behind growing anticlines only occurs in mountain belts, whilst capture of channels through complete submergence of inter-rill areas occurs at much smaller scales.

In addition to identifying the processes that control drainage basin shape and spacing, it is important to ascertain whether these two morphological features are determined during the early stages of drainage network growth. If this is the case, drainage basin shape and spacing may be unrelated to climatic or topographic parameters measured at the present day. In areas of active faulting this point is particularly important, as the initial stages of drainage development occur on low-gradient surfaces which are subsequently uplifted and tilted. This paper demonstrates the relative importance of the initial stages of drainage network growth using observations of drainage development on the Wheeler Ridge anticline in California.

DATA COLLECTION

Drainage basins on linear fault blocks may be subdivided into three fundamental types: (i) basins which reach the topographic ridge crest (i.e. 'ridge-pole' of Hovius, 1996) of the fault block; (ii) basins which extend significantly beyond the ridge crest; and (iii) basins which drain only the frontal part of the range. These three types of network may also be recognized in larger-scale mountain belts (Talling *et al.*, 1993; Hovius, 1996) and result in drainage basins with distinctly different sizes, shapes and topographic gradients. In this study and that of Hovius (1996) only dimensions associated with the first category of basins were measured. The relative size of alluvial fans reflects the importance of sediment supply from this type of drainage basin (e.g. maps of Denny, 1965, for Death Valley, California). Locations in which drainage networks have breached the ridge crest are relatively unusual and were excluded from this research. Such large drainage networks may, however, have a significant impact on the facies developed in adjacent sedimentary basins. Basins in the third category are steeper and have higher sediment yields but lower sediment discharges than the other types of adjacent drainage basins (Sinha & Friend, 1994). The spacing and shape of these smaller basins is primarily constrained by the spacing of adjacent larger basins.

Method

The measurement procedure closely follows that employed by Hovius (1996). Morphometric measurements of drainage outlet spacing, drainage basin shape and mean gradient were made from topographic maps with scales of between 1:24 000 and 1:250 000 (Table 1). Locations were chosen where there was linear topography generated by presently active faults (Figs 1 and 2). Linear topography was defined as occurring when the sinuosity of the mountain front (Keller & Pinter, 1996) was less than 1.09. The sinuosity was derived from the ratio of the length of the mountain front between two points to the distance between those points in a direct line (the scale of topographic map used is given in Table 1). In all cases the break in slope representing the position of the mountain front could be clearly determined from topographic maps. As sinuosity will vary with map scale (Bull & McFadden, 1977), care needs to be taken when comparing sinuosities from different map scales. Only channel networks which extended over 70% of the way from the mountain front to the drainage divide were included in the study (Fig. 1B). Rivers with confluences less than 2% of the way from the mountain front to the drainage divide were treated as separate drainage basins. Hovius (1996) used equvalent run-off distances of 90 and 2%. Uncertainty in locating the channel head of smaller fault-block drainages on topographic maps was the main reason for the change in the way the upper cut-off was defined. The distance along the mountain front between adjacent drainage basin outlets was measured (Fig. 1B), and termed the drainage outlet spacing (s). A mean value of these outlet spacings (S) was calculated for each mountain front. The standard deviation (σ) of the spacings about this mean value was also calculated (Table 1). The ratio of the mean outlet spacing (S) and the standard deviation (σ), expressed as a percentage (σ%), is used to show if the outlet spacings are regularly spaced (Table 1). The half-width of the fault block (w) was measured for each drainage basin from the mountain front to the ridge-crest drainage divide, in a direction perpendicular to the general trend of the mountain front (Fig. 1B). The topographic relief (h) between the ridge crest and the mountain front was also measured for each drainage baisn (Fig. 1B). Mean values of topographic half-width (W) and relief (H) were used to characterize each mountain front. The ratio of H and W of the drainage basins gave the mean gradient (A) of the drainage basins (Table 1). The ratio of the mean outlet spacing (S) and mean topographic width (W) was used to characterize the typical shape, or spacing ratio (R), of drainage basins along each mountain front (Table 1). Hence

$$R = W/S. \quad (1)$$

Spacing ratios (s) were also measured for individual

Table 1. Parameters defining fault-block morphology.

Location number	Tilt block name	Flank	Relief (H in m)	Half-width (W in km)	Gradient (A m km^{-1})	Spacing (S in km)	SD (σ in km)	SD (σ%)	No. rivers	Sinuosity	Map scale	Spacing ratio (R)	Spacing ratio (R'')	SD (σ'' in km)
Tilt Blocks														
	Nevada													
1	Tobin Range	East Side	735	3.08	239	1.20	0.450	38	11	1.008	1: 250 000	2.56	2.49	1.30
2	Stillwater Range	Dixie Valley	1014	4.39	231	1.70	0.630	37	16	1.011	1: 250 000	2.58	2.20	0.91
3	Humboldt Range	West Side	1274	5.30	254	1.92	0.954	50	13	1.009	1: 250 000	2.81	2.33	1.38
4	Humboldt Range	East Side	1349	6.62	201	4.71	0.580	12	7	1.010	1: 250 000	1.41	1.43	0.15
5	Clan Alpine Range	East Side	915	5.89	155	2.25	1.14	51	12	1.018	1: 250 000	2.62	3.23	1.51
6	Clan Alpine Range	West Side	1216	6.29	203	2.16	0.995	46	7	1.011	1: 250 000	2.91	3.5	1.40
7	Stillwater Range	West Side	1006	3.79	265	2.27	0.820	36	13	1.005	1: 250 000	1.67	1.87	0.94
8	Stillwater Range	Northeast Side	1117	5.90	189	1.90	0.930	49	6	1.008	1: 250 000	3.11	3.71	1.58
9	Sheep Range	(near Las Vegas)	1034	4.03	257	2.44	0.680	19	10	1.010	1: 250 000	1.65	1.72	0.28
10	Toiyabe Range	East Side	1147	3.83	299	1.53	0.640	42	10	1.006	1: 250 000	2.50	2.50	0.72
11	Toiabe Range	West Side	1084	7.87	138	4.29	3.19	74	7	1.021	1: 250 000	1.82	5.64	3.88
	California													
12	Penamint Range	Southwest Side	2092	11.5	181	3.42	1.42	42	7	1.014	1: 250 000	3.37	3.12	0.77
13	Penamint Range	Southeast Side	2414	11.1	218	4.65	1.54	33	6	1.013	1: 250 000	2.38	2.26	0.58
14	White Mountain	West Side	2198	7.82	281	2.72	1.09	40	20	1.009	1: 250 000	2.88	2.73	1.92
15	White Mountain	East Side	2323	11.8	197	4.70	1.81	39	6	1.015	1: 250 000	2.51	1.72	0.45
19	*Colorado*													
16	Sangre Del Cristo Mt	West Side	1529	7.00	218	3.00	1.37	46	6	1.007	1: 250 000	2.33	2.93	1.44
17	Sangre Del Cristo Mt	Southwest Side	973	4.26	230	1.48	1.14	74	15	1.013	1: 250 000	2.88	4.55	3.17
	Idaho													
18	Pahsimeroi Mtns	West Side	665	2.70	246	1.05	0.670	64	11	1.008	1: 250 000	2.57	3.36	1.64
19	Lemhi Range	West Side	1118	5.36	209	2.96	1.21	41	8	1.013	1: 250 000	1.81	2.17	0.99
20	Lemhi Range	East Side	861	5.34	161	2.88	2.05	71	15	1.037	1: 250 000	1.85	4.03	3.70
Growth Folds														
	California													
21	Kettleman Hills	Mid dome-west side	64	2.29	28	0.670	0.280	42	9	1.005	1: 31660	3.42	3.89	1.21
22	Kettleman Hills	Mid dome-west bend	93	1.99	47	0.790	0.400	51	9	1.086	1: 31660	2.52	3.91	3.57
23	Kettleman Hills	N. dome-west side	69	3.18	22	1.29	0.700	54	8	1.005	1: 31680	2.47	3.34	2.11
24	Kettleman Hills	N. dome-farnorth sd	101	1.97	51	0.560	0.300	54	10	1.006	1: 31660	3.52	5.36	3.86
25	Kettleman Hills	N. dome-NE side	160	4.45	36	2.75	1.64	60	6	1.007	1: 31660	1.62	2.59	2.23
	Nepal													
26	Dundwa Range	North Side	612	6.45	94	2.20	0.700	32	11	1.007	1: 250 000	2.93	3.14	0.78
27	Dundwa Range	South Side	721	5.76	130	2.72	1.34	49	18	1.017	1: 250 000	2.12	2.74	1.51
28	Range west of the	Girwa River	1178	5.65	209	1.39	0.540	39	19	1.010	1: 250 000	4.06	4.84	2.24
29	Churia Range	S. of Babai River	734	3.77	195	1.74	1.16	67	44	1.021	1: 250 000	2.17	2.81	1.42
30	Churia Range	N. of Babai River	1057	3.69	286	1.66	0.830	50	39	1.019	1: 250 000	2.22	2.89	1.17
31	Chandigarh Dun	South Side	210	7.93	26.5	2.48	0.860	35	13	1.021	1: 50 000	3.20	4.05	2.82
Old Topography														
	Appalachians													
32	River Mountains	South Side	124	0.530	234	0.340	0.270	79	13	1.021	1: 24 000	1.56	2.56	1.67
33	Goshen Mountains	North Side	174	0.520	335	0.210	0.0900	43	20	1.024	1: 24 000	2.48	2.79	1.04
34	Goshen Mountains	South Side	151	0.370	408	0.180	0.110	61	22	1.018	1: 24 000	2.06	3.18	2.23
35	North McGee Mountain	South Side	161	0.880	183	0.610	0.0700	11	7	1.017	1: 24 000	1.44	1.99	1.51
36	McGee Mountains	North Side	209	0.490	427	0.200	0.0800	40	16	1.007	1: 24 000	2.45	2.51	1.18
37	McGee Mountains	South Side	174	0.530	328	0.260	0.0700	27	14	1.014	1: 24 000	2.04	2.29	0.91
38	Bays Mountain	North Side	270	0.960	239	0.960	0.630	66	6	1.011	1: 24 000	1.18	1.96	1.41
39	Bays Mountain	South Side	262	0.880	298	0.250	0.100	40	16	1.006	1: 24 000	3.52	4.44	3.06
Nonlinear Mtn. Front														
	Nevada													
40	Shoshone Range		849	6.31	135	4.02	1.94	48	14	1.098	1: 250 000	1.57	1.87	0.91
41	Sonoma Range		949	7.46	127	5.18	3.18	61	7	1.102	1: 250 000	1.44	1.31	0.59
42	Fox Range		645	5.18	125	3.93	3.82	97	11	1.189	1: 250 000	1.31	2.23	1.26
43	East Range		567	5.38	105	4.56	2.67	59	13	1.225	1: 250 000	1.18	1.57	1.04

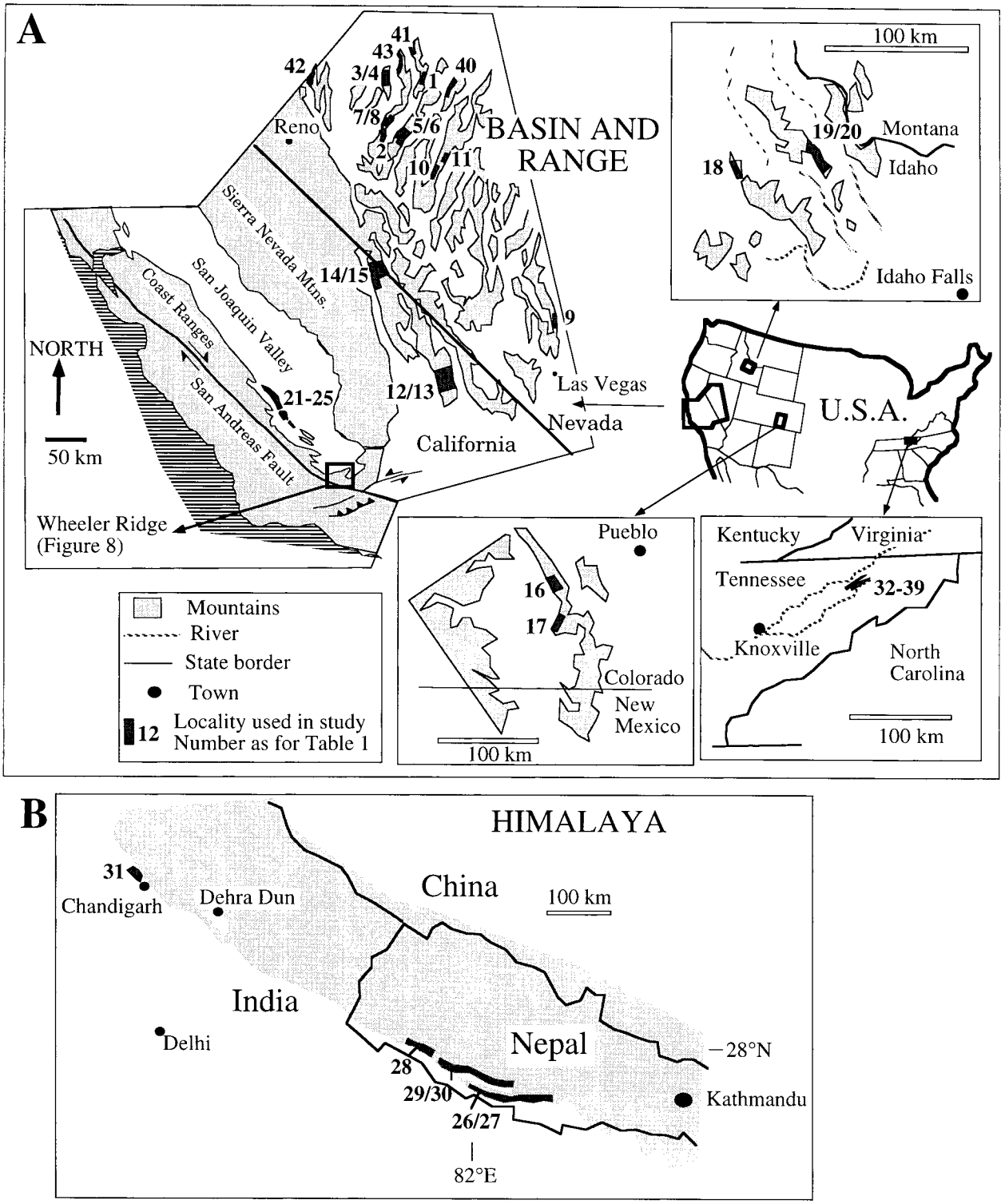

Fig. 3. Map showing the locations at which drainage outlet spacings were measured (A) in the western USA, and (B) in the frontal Himalaya in India and Nepal. Numbers shown next to the localities refer to Table 1.

drainage basins along each mountain front (Table 2). The mean of each mountain front's spacing ratios (R'') and its standard deviation (σ'') were calculated (Table 1). The value of R'' is typically greater than the value of R for the same mountain front. This discrepancy is due to the mean value of $1/s$ being greater than $1/S$, where S is the mean value of s. The mean value of w/s is thus greater than the ratio of the mean values of width and spacing (W/S).

The value of R is used in this study to characterize the fault block spacing ratio, as this allows comparisons to be made to mountain belt spacing ratios which were

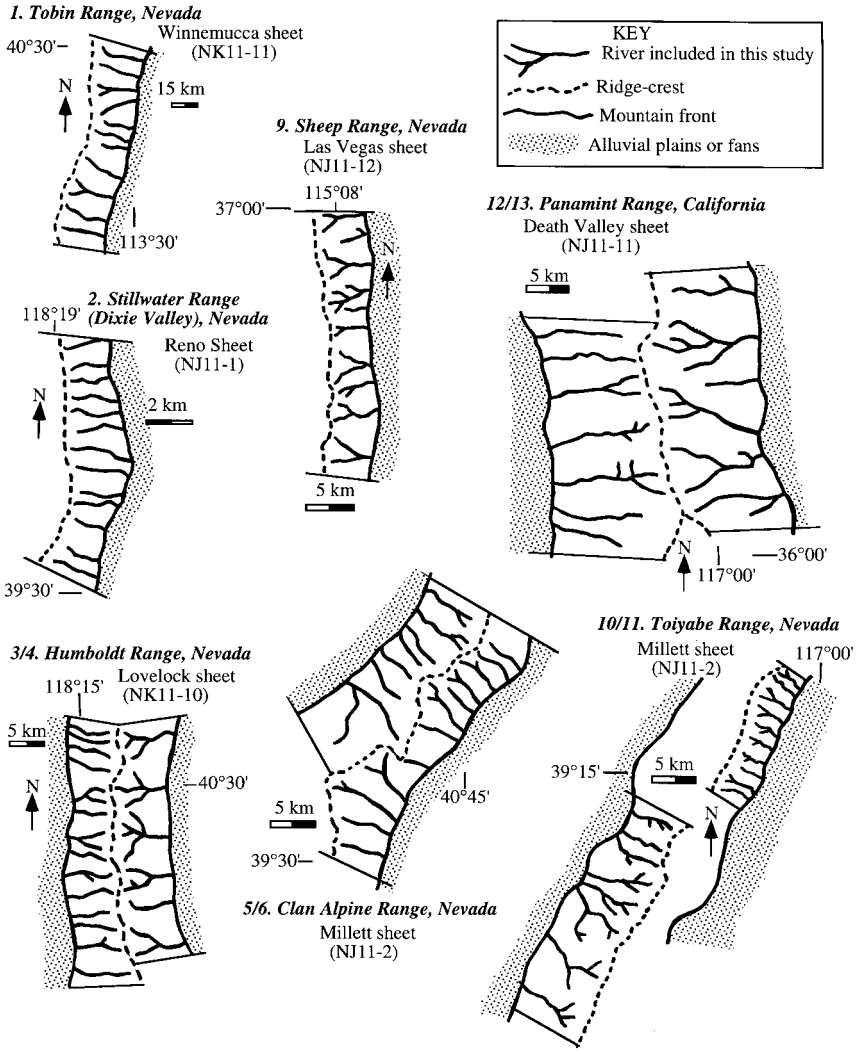

Fig. 4. Drainage networks used to calculate mean outlet spacing and spacing ratios (redrawn from topographic maps). Location numbers refer to those given in Table 1 and Fig. 3.

calculated by Hovius (1996) in the same way. The degree of regularity in outlet spacing (S/σ) is subsequently discussed in this study, as this directly determines the spacing of alluvial fan apices. The degree of regularity in spacing ratios (R''/σ'') is also shown in Table 1.

Tectonic setting of fault blocks

Drainage basin spacings were measured on one or both sides of 12 tilt blocks generated by extensional faulting in the tectonically active Basin and Range province in the western USA (Fig. 3A). This resulted in measurements along 20 individual mountain fronts (Table 1). Faulting in Nevada and Idaho began between 10 and 4 Ma (Scott *et al.*, 1985; Okaya & Thompson, 1985) and is presently active (e.g. Crone & Machette, 1984; Bell & Katzer, 1990). Particularly well-defined mountain fronts are typically coincident with major extensional faults (e.g. Wallace, 1978; Leeder & Jackson, 1993). In central Nevada and Idaho drainages were superimposed on relatively flat surfaces covered by basaltic lava flows (Okaya & Thompson, 1985; Leeder & Jackson, 1993).

Data were also collected for drainage basins on seven anticlinal folds uplifted by thrust faults. Four of these anticlines are located at the front of the Himalaya mountain belt in India and Nepal (Fig. 3B). The Himalayan anticlines are asymmetric with large faults interpreted to crop out at the base of their southern flanks (Yamanaka & Yagi, 1984; Corvinus, 1990; Kumar, 1993). Faulting initiated between 2.5 and 0.5 Ma (Ranga Rao, 1986; Corvinus, 1990; Appel *et al.*, 1991), and continues at the present day (Yeats & Lillie, 1991). Three anticlines constituting the Kettleman Hills in the San Joaquin Valley, central California, were also considered (Fig. 3A). These anticlines have been uplifted by blind thrust faulting since 8 Ma (Woodring *et al.*, 1940). A magnitude 6 earthquake was recorded below the Kettleman Hills in 1985 (Ekstrom *et al.*, 1992).

The current climate and vegetation types found in the western United States and the frontal part of the

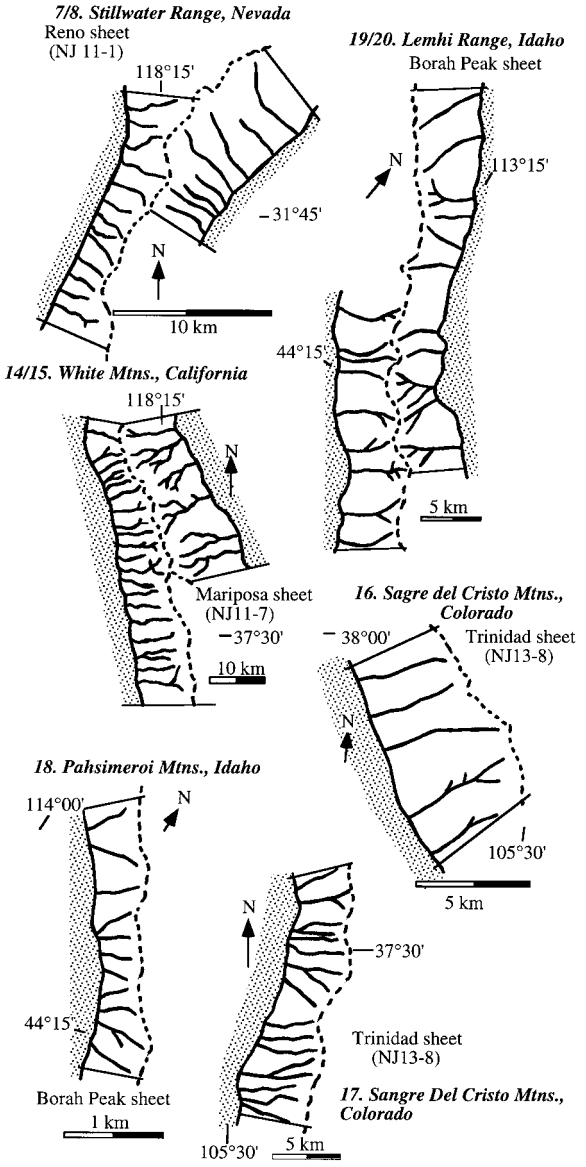

Fig. 4. (*continued*).

Himalaya are very different. Mean annual rainfall is less than 400 mm in the predominantly semiarid climate of the western United States (Bryson & Hare, 1981), whilst rainfall exceeds 1000 mm for the dry tropical and monsoonal climate of the frontal Himalaya (Takahashi & Arakawa, 1981). The two areas are also likely to have experienced very different climates in the past.

Nonlinear and ancient topography

Measurements of mean outlet spacing (S), topographic half-width (W), relief (H) and gradient (A) were repeated for four nonlinear mountain fronts in the Basin and Range province (Figs 3A and 4) with sinuosities of up to 1.225 (Table 1). These data allow the effects of increased sinuosity on drainage evolution to be addressed. Measurements were also taken for linear mountain fronts on old topography in the Appalachians (Figs 3A and 4; Table 1). The linear nature of this topography reflects linear outcrop of bedrock lithologies. Thrust faulting which initially formed the Appalachian mountain belt ceased in the late Palaeozoic, although the area has been affected by later tectonic events (Gardner & Sevon, 1989). Appalachian drainage networks are thus much older that the other networks considered in this study. The effects of drainage age on drainage basin character can thus be considered.

RESULTS

The data support the qualitative observation that there is a degree of regularity in the spacing of drainage basin outlets on the flanks of linear fault blocks. In 25 of the 31 locations on fault blocks the standard deviation of the outlet spacings (σ) is less than 55% of the mean outlet spacing (S) (Fig. 5A). Although the number of drainage outlets measured along each mountain front varied between 5 and 43 (Table 1), there is no significant correlation between a lower number of outlets measured and a higher standard deviation. The standard deviation (σ) increases as the mean outlet spacing increases (Fig. 6B), which prompted the use of a standard deviation normalized by this mean spacing (σ%). A similar degree of regularity in outlet spacing was documented for mountain belts (Fig. 5A; Hovius, 1996). Drainage outlets were less regularly spaced on fault blocks with a sinuosity greater than 1.09, with the standard deviation rising to between 48 and 97% of the mean outlet spacing (Fig. 6A).

Although there is a high degree of regularity in outlet spacings along each individual fault block, the mean value of the drainage basin spacing ratios (R) is highly variable (Fig. 5). Spacing ratios vary between 1.41 and 4.06 for different fault blocks (Table 1). Such variability is greater than the uncertainties involved in measuring the spacing ratios (Appendix 2). No correlation is seen between spacing ratios of fault blocks, their present-day topographic gradient (Fig. 7) or relief and mountain front sinuosity. The spacing ratio was also found to be statistically unrelated to the half-width of the fault block, even though the half-width was used to calculate the spacing ratio. The variability in spacing ratios of fault blocks is much grater than theat seen for mountain belts (Fig. 5; Hovius 1996; Talling *et al.*, 1993). The average spacing ratio of 2.5 for fault blocks is also significantly greater than the mean of 2.1 for mountain belts.

Drainage outlets from mature Appalachian drainage basins on linear topography were found to have a similar deree of regularity to those on linear fault blocks and mountain belts (Fig. 5). The spacing ratios of Appalachian drainage basins range between 1.2 and 3.5, with a similar average to that for mountain belts of 2.1 (Table 1; Fig. 5).

Local factors causing low spacing ratios

Unusually low spacing ratios observed on two fault blocks can be directly attributed to particular local factors.

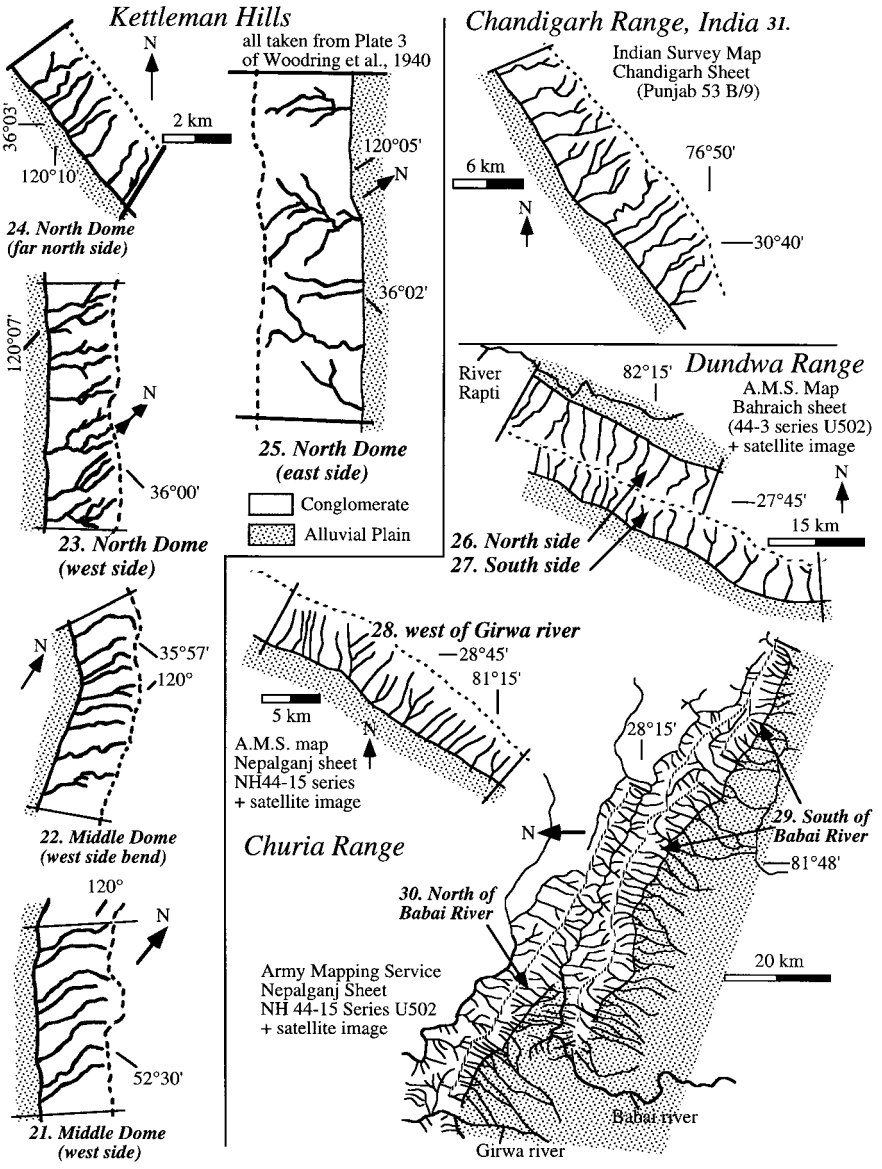

Fig. 4. (*continued*).

Erosion of the Kettleman Hills has resulted in ridges of resistant conglomeratic lithologies orientated parallel to the mounatin front (Fig. 4; Woodring *et al.*, 1940). Rivers draining the northern flank of the Kettleman Hills are deflected by these ridges to produce relatively square drainage basins with a low spacing ratio (Figs 4 and 7). These drainage patterns are similar to those produced by diversions behind the frontal anticlines of the Nepali Himalaya. Extensional faulting along the eastern side of the Humboldt Range has migrated to a fault located closer to the mountain crest (Wallace, 1978). This migration abruptly dereased the half-width of topography and increased the spacing ratio (Figs 4 and 7). Changes in fault-block half-width are likely to have occurred in other locations during the growth of both extensional and compressional fault systems (e.g. Leeder & Jackson, 1993; Wallace 1978; Suppe, 1983). If these two locations are treated as anomalous, the range of spacing ratios for fault blocks is slightly reduced to between 1.67 and 4.06 (Fig. 6B).

DRAINAGE DEVELOPMENT AT DIFFERENT SCALES

The outlet spacing and spacing ratios observed on fault blocks may be compared to similar quantitative data from mountain belts (Hovius, 1996; Talling *et al.*, 1993) and flume experiments (Mosley, 1972; Schumm *et al.*, 1987). This comparison allows us to compare drainage evolution in large- and smaller-scale systems, and on static or progressively uplifted surfaces. Differences in the drainage basin form may be used to interpret changes in the physical processes which operate in each setting, and hence provide insights into the basic processes affecting drainage evolution.

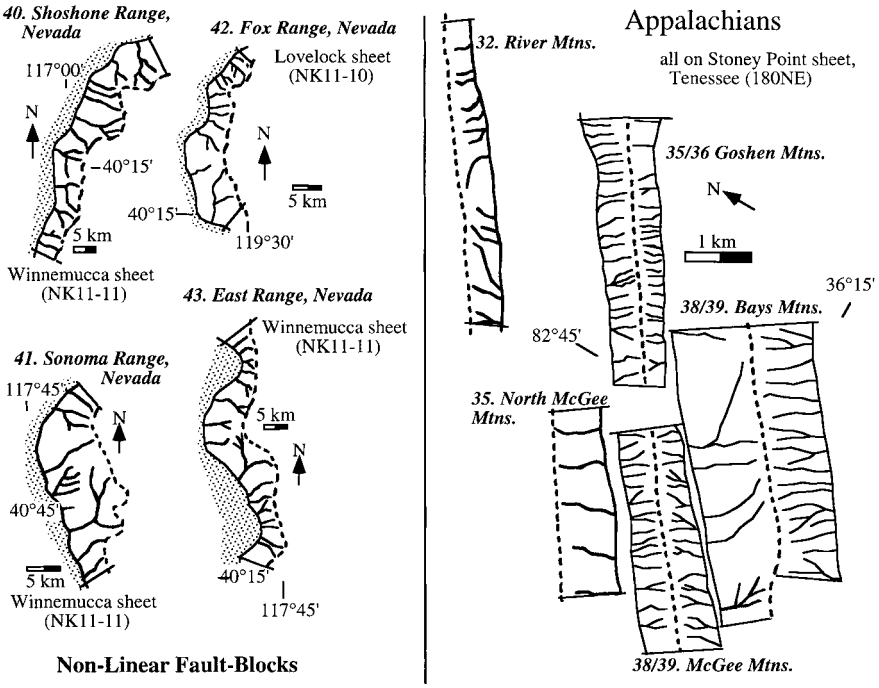

Fig. 4. (*continued*).

Experimental growth of small-scale drainage networks

Mosley (1972) reported that drainage networks created experimentally in a 10 by 15-m container of sand showed higher spacing ratios on higher gradient surfaces (Schumm *et al.*, 1987). In these experiments rainfall was simulated by a sprinkler system and drainage networks were developed on a planar surface whose initial slope was varied between 22 and 121 m km^{-1}. Spacing ratios varied between 3.6 and 10.0. Leeder (1991) and Leeder & Jackson (1993) suggest that these experiments indicate that drainage basins with higher spacing ratios will form on extensional tilt blocks with higher present-day slopes. This study does not support such a conclusion. No correlation was observed between the present-day gradients of tilt blocks or growth folds and the spacing ratios (Fig. 7). Discrepancies between the experimental results and the data presented in this study indicate fundamental differences in how drainage networks evolve on (i) two different spatial scales and (ii) progressively uplifted or static surfaces. Certain processes which affect experimental drainage evolution on scales of up to 10 m, such as capture between adjacent channels by complete overflooding of intervening topography, do not affect drainage evolution on tilt blocks and growth folds (Fig. 8). As subsequently illustrated using observations from the Wheeler Ridge, drainage development on fault blocks is strongly influenced by topographic slopes present during initial drainage development. Owing to progressive uplift and tilting, these slopes may by quite different to those seen at the present day. It is likely that the gradient of these initial slopes strongly affects the spacing ratio subsequently observed. Both of these points suggest that caution needs to be exercised in interpreting how large-scale drainage networks develop using small-scale flume experiments.

Mountain belts

Mountain belts are produced by a more complex history of deformation than fault blocks, with uplift occurring above multiple faults. The mountain belt studies by Hovius (1996) typically have half-widths of between 20 and 40 km, although two of his 11 localities have half-widths of $\approx$85 km. With the exception of one locality with a half-width of 18.2 km, half-width of fault blocks range between 1.9 and 13 km (Table 1). The southern Alps of New Zealand illustrate the continuum between fault blocks and mountain belts. It is the narrowest mountain belt (W=21.1) included in Hovius's study, and has been predominantly uplifted by a single transpressional fault (Walcott, 1978).

The remarkably constant spacing ratios for mountain belts (Hovius, 1996) are much less variable than those observed on fault blocks (Fig. 6B). It is inferred that local variations in factors affecting drainage evolution cause such variability, whilst over the larger scale of mountain belts local variations become less important (Fig. 8). The exact nature of the local factors causing the variability in fault block spacing ratio is enigmatic, as there is no simple relationship between a single factor and the spacing ratio. Variations in spacing ratios do not correlate with the geographical location of the fault block (Fig. 7), even though climate (including rainfall and temperature), vegetation, tectonic history and age of

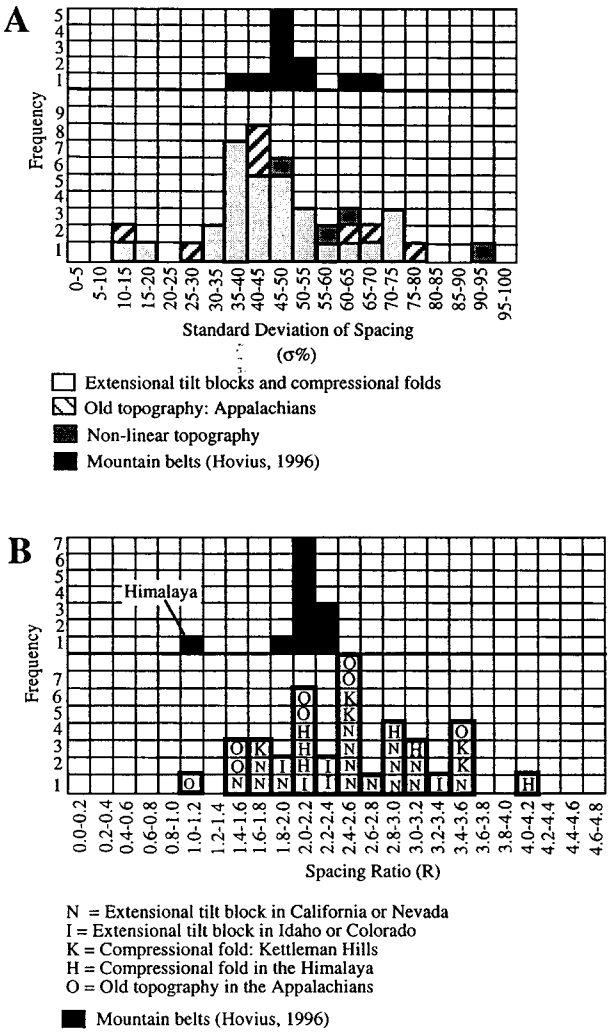

Fig. 5. Histogram showing the frequency of (A) the standard deviation of the outlet spacings expressed as a percentage of the mean outlet spacing (σ%), and (B) the spacing ratio (R). Data from faults in blocks in different geographical locations are indicated, together with data from mountain belts (Hovius, 1996), Appalachian drainage basins, and nonlinear fault blocks.

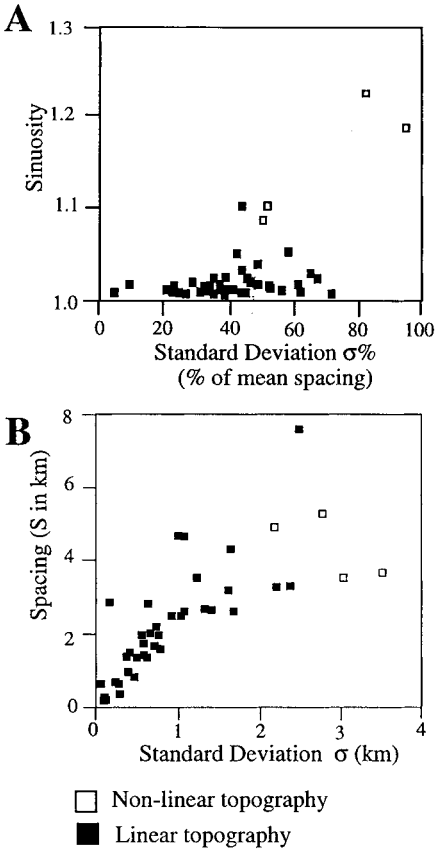

Fig. 6. (A) Plot showing the relationship between the standard deviation of outlet spacings, expressed as a fraction of the mean spacing, and the mountain front sinuosity. Solid circles refer to the nonlinear tilt blocks listed in Table 1. (B) Plot showing the positive correlation between the mean outlet spacing (S) along the mountain front, and the standard deviation of that spacing.

uplift vary significantly between locations in the Himalaya and western USA. Variations in present-day gradients also fail to affect spacing ratios (Fig. 7). The relative consistency of mountain belt spacing ratio may be explained as being due to the greater erosive power available to large rivers within mountain belts. This increase of the notional ratio of stream erosion to rates of tectonic uplift allows these drainage basins to reach an optimal shape with a spacing ratio of ≈ 2 despite a complex spatial pattern of tectonically driven uplift.

The mean spacing ratio for active growth folds and tilt blocks of 2.5 is significantly higher than the mean of 2.1 for mountain belts and mature Appalachian drainage networks (Fig. 6B). Thus, the mean shape of drainage basins in orogens tends to be less elongate. During the evolution of drainage networks capture events have the potential to increase the spacing of drainage outlets, and hence make the drainage basin shape less elongate. In contrast, increases in the spacing ratio due to the initiation of new drainage networks is unlikely. It is speculated that this lower mean spacing ratio for mountain belts reflects the increased likelihood of major capture events. Drainage patterns parallel to the mountain front, which might be expected to result from capture events behind structural uplifts, are rare, however, in the mountain belts studied by Hovius (1996). Computer modelling of drainage evolution could provide a way to determine how spatially irregular uplift patterns involving multiple fault blocks can produce such a uniform spacing ratio.

IS OUTLET SPACING DETERMINED DURING INITIAL GROWTH?

Observations of drainage evolution on the Wheeler Ridge anticline in the San Joaquin Valley of central California, USA, suggest that drainage outlet spacing is primarily determined during the early stages of channel network growth (Fig. 9). Drainage networks on surfaces uplifted by a blind thrust fault during the last 14 kyr (Zepeda *et al.*, 1998; Mueller & Talling, 1996) have already reached locations close to the ridge crest and channel

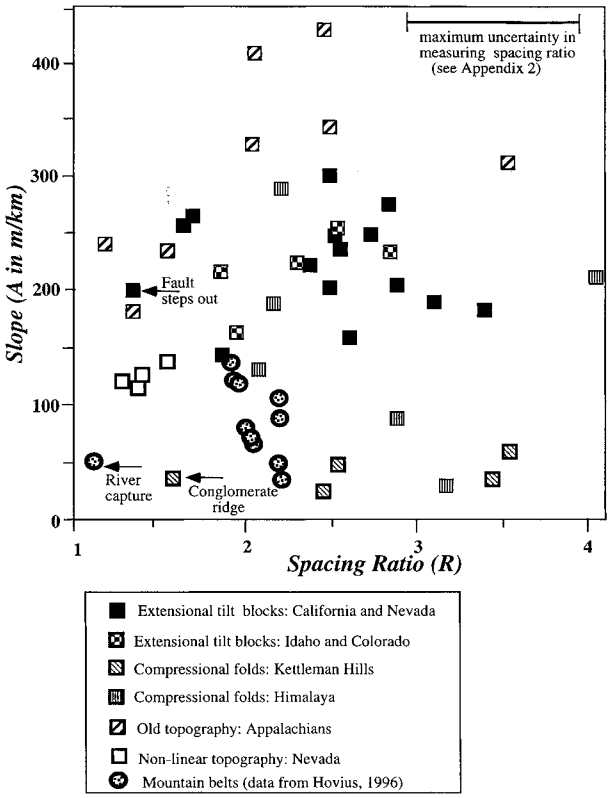

Fig. 7. Plot showing the lack of correlation between spacing ratio and gradient for fault blocks and mountain belts (data from Hovius, 1996). The geographical location of fault blocks is indicated. Three sites whose spacing ratio has been reduced by specific local factors (see text) are indicated by arrows. Estimates of the uncertainty of $\pm 20\%$ in measuring the spacing ratio (R) are derived in Appendix 2.

incision has produced significant topographic relief (Fig. 9). It seems unlikely that either of the two drainage networks that reach the ridge crest (networks A and C in Fig. 9) will be removed by capture events, or that additional channel networks will reach the ridge crest. The number and spacing of major drainage basins appears to have been determined during the first 14 kyr of network growth. An absence of field data documenting large-scale drainage capture events on other fault blocks, together with process-based computer simluation of drainage growth (e.g. Howard, 1994), also imply that the number and spacing of drainage outlets reaches a stable value during the early stages of drainage growth. If river channels which are originally lightly etched into the landscape subsequently remain fixed, the rate at which channels incise must be greater than the rate at which hillslopes are denuded. The lack of correlation between outlet spacing or spacing ratios and parameters measured at the present day (e.g. slope or climate) may be a result of this dependence on the initial stages of drainage growth. Variable topographic gradients and rates of tilt during initial drainage growth may have produced the variations in spacing ratio measured at the present day. A positive correlation between spacing ratio and slope, as seen in flume experiments (Schumm *et al.*, 1987), may indeed occur during the early stages of drainage network growth.

Computer models (e.g. Howard, 1994), small-scale field studies (Schumm, 1956; Morisawa, 1964) and flume experiments (Schumm *et al.*, 1987) have shown that microtopography on the initially uplifted surface strongly affects the location at which channels subsequently form. It might be inferred that essentially random microtopography on the initial surface has produced the observed scatter in spacing ratios for fault blocks. The computer model of Howard (1994), however, indicates that although initial microtopography may dictate where individual channels occur it has little effect on the average morphology (e.g. hypsometric curves) of larger scale landscapes. It is also difficult to explain how initial microtopography produces variable spacing ratios on fault blocks but not for orogens.

PROCESSES OF DRAINAGE EVOLUTION

Drainage networks on Wheeler Ridge suggest that two important processes determine the spacing of drainage outlets of basins reaching back to the ridge crest (Figs 9 and 10). First, a critical drainage area is needed to produce a channel head. Recent work has shown that on low gradients (≈ 100 m km^{-1}) this area is inversely related to the local gradient at the channel head (Montgomery & Dietrich, 1992). If this drainage area is similar for adjacent channel heads, equally spaced channel networks will be formed during the earliest stages of channel growth (Fig. 10). It is tempting to infer that the regularity of drainage outlet spacing observed in mature drainage networks is related to this equal spacing. The factors determining the critical area needed for a channel head (slope, precipitation, runoff efficiency, vegetation, substrate lithology) are likely to be similar for adjacent areas on each fault block, but vary significantly between fault blocks. In such a model, variations observed in spacing ratios on fault blocks would be produced by these factors influencing the critical area. If such a model was valid, however, drainage basin outlet spacing (S) would be independent of the length of the drainage basin (W). Drainage outlet spacing is shown by this study to be strongly correlated with drainage basin length (Fig. 11A). Although variations in the critical area needed to initiate a channel may influence spacing ratios, they cannot be a dominant control. It appears that the second process illustrated by the drainage basins on the Wheeler Ridge, the competition between adjacent channel networks subsequent to their initiation (Figs 9 and 10), may be of crucial importance. This process may itself be split into elongation of channels towards the drainage divide and subsequent widening of the drainage basin in response to downcutting by this channel. Drainage basins A and C on the ridge (Fig. 9) have extended to near the ridge crest and truncated the growth of the shorter drainage basin B. It appears that once drainages A and

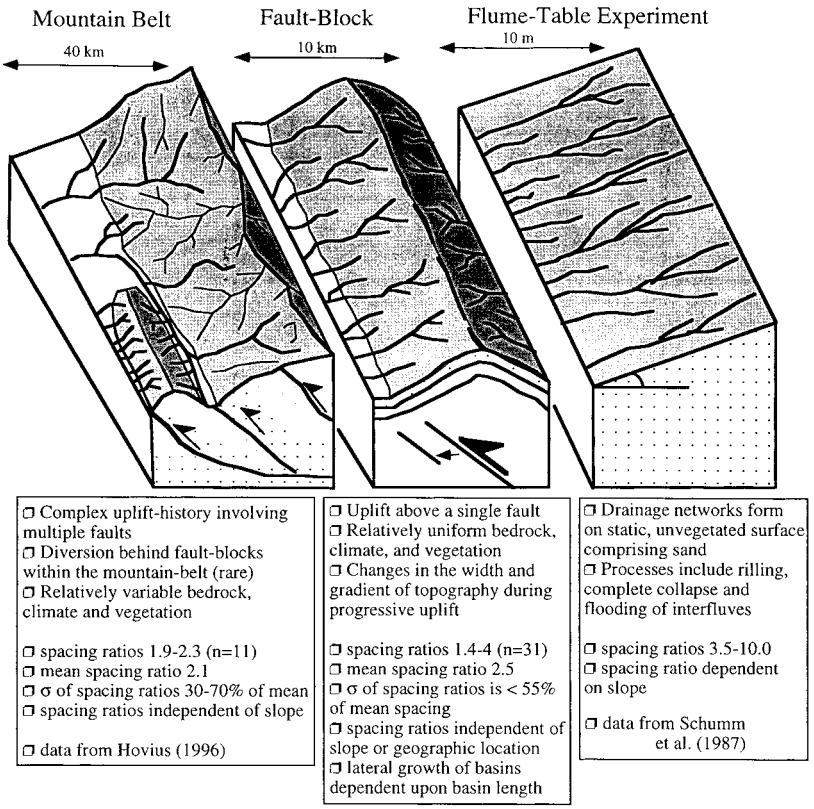

Fig. 8. Schematic drawings summarizing the different processes affecting drainage network growth in mountain belts, on fault blocks and in flume-table experiments.

C extended beyond drainage B, they captured sufficient drainage area from drainage B to prevent its headward extension (Fig. 9).

Drainage networks on Wheeler Ridge also suggest that rates of tilting during the earliest stages of network growth may strongly affect how a drainage basin widens in competition with its neighbouring basins. The northern flank of the ridge is considerably steeper than the southern flank, and has undergone more rapid uplift and tilting (Fig. 9). Channels on the steeper flank have extended towards the drainage divide more rapidly, producing relatively elongate drainage basins. These channels have incised quickly due to their higher gradients. Presumably, such rapid channel incision will favour future preservation of the elongate drainage networks with high spacing ratios. The correlation between higher slopes and higher spacing ratios in flume experiments may originate in a similar way (Mosley, 1972; Schumm *et al.*, 1987). Computer modelling of drainage network initiation on tilting surfaces (*q.v.* Howard, 1994) and improved field data constraining fault block uplift rates could improve our understanding of the influence of variable rates of surface uplift.

The length of drainage basins on the Wheeler Ridge anticline is determined by the width of topographic uplift by subsurface faulting. It is the lateral growth of drainage basins, and the processes which determine the extent of that growth, which can produce the final spacing ratio (Figs 9 and 10). This study shows that the width of drainage basins (S) increases as the tectonically determined length of the basins (W) increases (Fig. 11a). Thus, the processes determining basin width are affected by the length of topography upon which the basins develop. It is speculated that during initial extension of the drainage network towards the ridge crest, a wider fault block favours greater lateral growth of drainages and the beheading of a greater number of intervening drainages (Fig. 10). Changes in the half-width of extensional fault blocks and compressional growth folds are likely to occur during their progressive uplift (e.g. Wallace, 1978; Suppe, 1983; Leeder & Jackson, 1993). Such changes will alter the fault block spacing ratios, and may be a significant source of variability in the presently observed spacing ratios.

IMPLICATIONS FOR BASIN-FILL ARCHITECTURE

The spacing ratio allows the characteristic length-scale of facies variations (Fig. 2) to be predicted if the length of topography is known (Hovius, 1996; Allen & Hovius, 1998). However, it should be noted that rivers originating from beyond the ridge crest, which are not included in this study, often play an important role in determining facies patterns in fault-bounded basins. The width of topography present during active faulting can be estimated from relatively detailed seismic reflection profiles (e.g. Pieri & Groppi, 1981). The total width of the fault block at a given time is the distance between the points at which sediment onlaps the fault block. The location of the topographic crest of the fault block may then be estimated using the fault block's shape. Estimating fault-

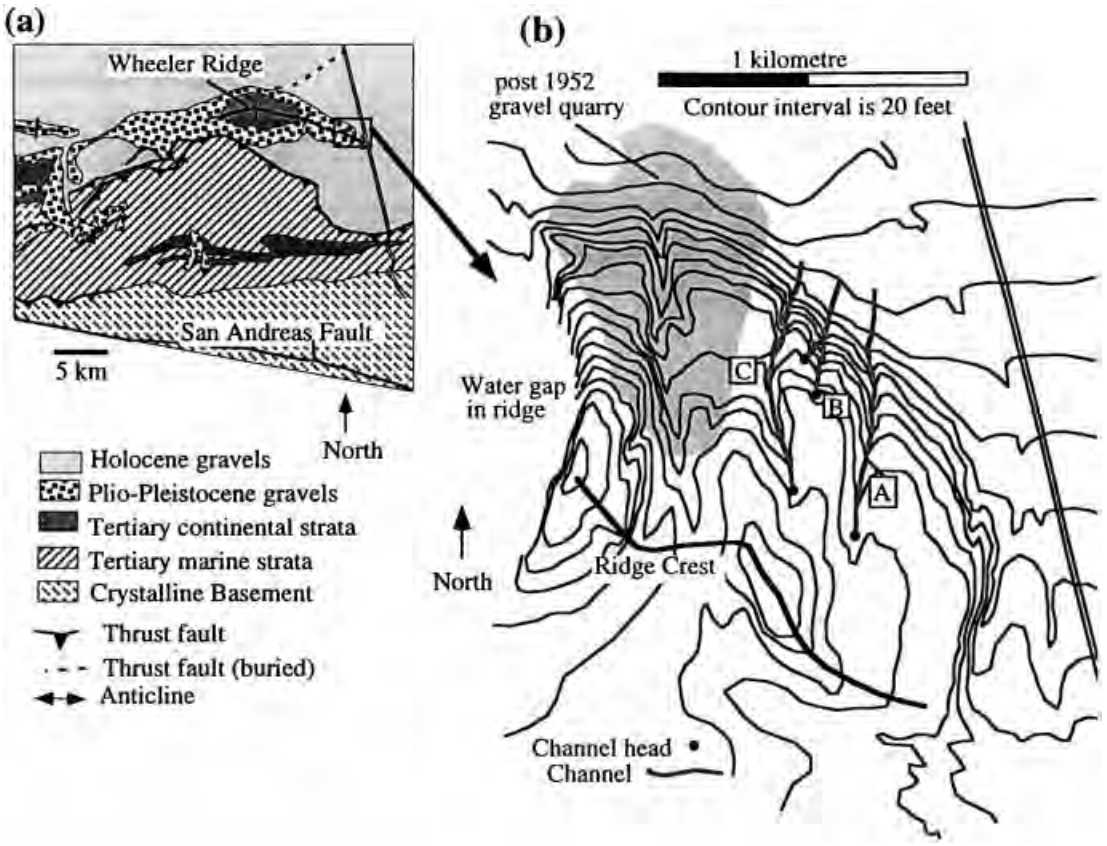

Fig. 9. (A) Location map showing the position of the Wheeler Ridge anticline in California. (b) Drainage networks observed on a surface uplifted during the last 14 kyr at the ridge's eastern terminus (Mueller & Talling, 1996; Zepeda *et al.*, 1998). The position of channel heads for channel networks A, B and C is based upon field observations in 1993. Contours are redrawn from a 1 : 24000 scale USGS topographic map. There is a wind-gap, representing the location at which a river once flowed across the ridge, in the vicinity of the quarry. As the wind-gap strongly influenced later drainage development, the drainage basin to the west of channel C is not included in this study.

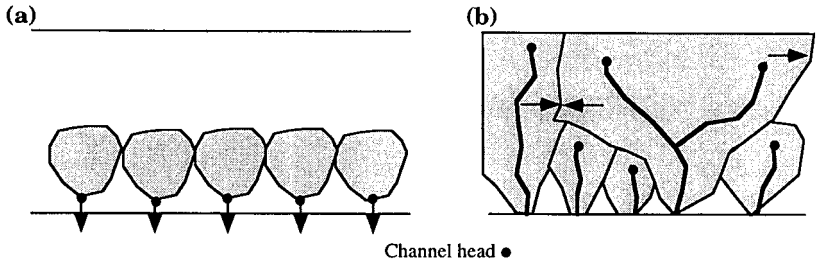

Fig. 10. Schematic illustration, based on observations at the Wheeler Ridge (Fig. 9), showing the two fundamental processes affecting the position of drainage outlets. Channel heads initially form where the product of local gradient and upstream area is sufficiently great. These channel heads will be regularly spaced on approximately planar topography. Drainage basins subsequently expand laterally as they extend towards the drainage divide. A few large drainage basins behead one or more intervening basins, until a stable drainage pattern is reached. It is this latter stage of drainage evolution that primarily determines the spacing ratio of the fault block.

block half-width in areas without seismic reflection data would be significantly less precise. Predicting the length scale of lateral facies variations is of critical importance in the development of petroleum reservoir units (e.g. papers in Flint & Bryant, 1993). Alternatively, if the separation of alluvial fan apices can be determined in ancient strata, the width of adjacent topography may be estimated. Hovius (1996) provides an example in which the spacing of late Oligocene fan apices in the North Alpine foreland basin is used to estimate the half-width of the adjacent orogen. The variability of spacing ratios (1.4–4) on fault blocks does not allow such precise prediction of the scale of lateral facies variation or topographic half-widths. For instance, reasonable mean outlet spacings for a fault block with a half-width of 5 km range from 1.25 to 3.6 km. This variability would be added to by the scatter of individual outlet spacings about a mean value. The more consistent spacing ratios

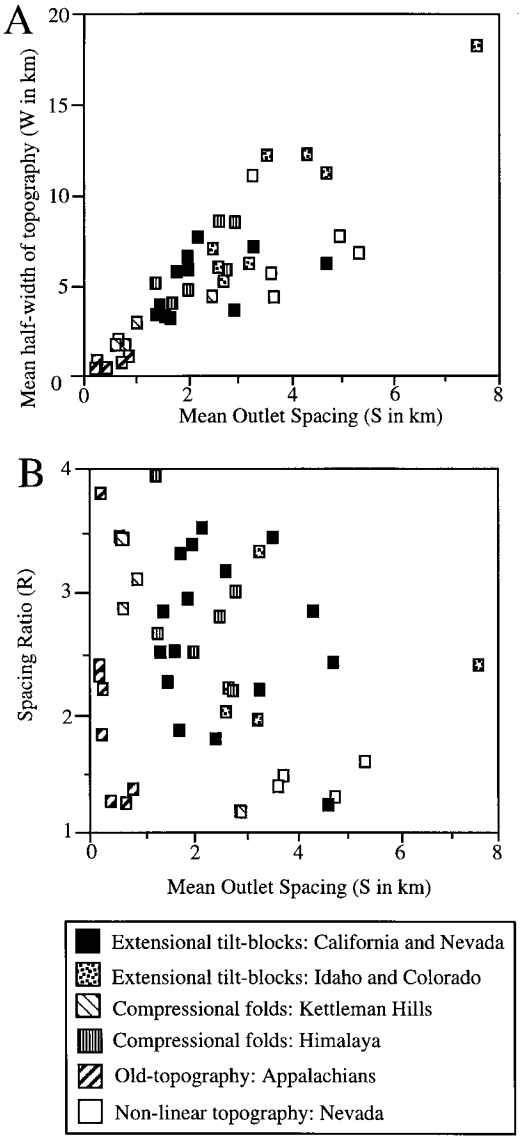

Fig. 11. Plots showing the relationship between the mean outlet spacing (S), the average half-width of topography (W) and the spacing ratio (R).

observed in mountain belts (Hovius, 1996) allow much more precise predictions to be made. An understanding of the factors influencing the spacing ratio on fault blocks would improve the precision of the estimate, although determining such factors for ancient fault blocks is likely to be problematic.

CONCLUSIONS

There is significant regularity in the spacing of drainage outlets on linear fault blocks. This regularity is such that the standard deviation of the spacing is typically less than 55% of the mean spacing. This degree of regularity is similar to that observed in the spacing of drainage outlets from linear mountain belts (Hovius, 1996).

The characteristic spacing of drainage outlets on individual fault blocks results in a characteristic drainage basin shape or spacing ratio (R) for that fault block. The spacing ratio for fault blocks varies between 1.4 and 4.1 This variability greatly exceeds that observed for linear mountain belts, whose spacing ratios range from 1.9 to 2.3.

No correlation is seen between the spacing ratios from fault blocks and their present-day slope. A strong correlation between spacing ratio and slope is observed for drainage networks produced in 10-m-scale flume table experiments on unvegetated surfaces which are kept at a constant slope during a single experiment (Mosley, 1972; Schumm *et al.*, 1987). This suggests that there are fundamental differences in the processes affecting drainage evolution on (i) different length scales and (ii) static or progressively uplifted surfaces.

Drainage evolution on the Wheeler Ridge anticline suggests that the outlet spacing is largely determined during the early stages of network growth on relatively low slopes. This dependency on initial conditions may explain the lack of correlation between spacing ratios and parameters measured at the present day (e.g. slope).

Variability in fault block spacing ratios is attributed to factors influencing the spacing of channel heads and rates of channel incision during the earliest stages of network growth, together with subsequent widening or narrowing of the fault block due to fault migration. Factors such as uplift rate, precipitation, runoff, vegetation and substrate resistance are likely to be similar for adjacent drainage basins on the same fault block, but vary significantly between fault blocks. Further work is needed to identify the exact role of these factors as there is no correlation between spacing ratios and the geographical location of fault blocks. This suggests that there is no simple relationship between spacing ratio and single geographically variable factors such as climate, vegetation or tectonic setting. Further work is also needed to determine why the spatially irregular uplift of multiple fault blocks in mountain belts produces relatively uniform spacing ratios, as processes such as mountain belt widening may be expected to produce variable spacing ratios.

Tectonic uplift patterns externally define the half-width of fault blocks (W). It is the lateral width of the drainage basins (s) which can be adjusted by erosional processes to produce the observed spacing ratios. A correlation is seen between wider drainage basins (s) and wider fault blocks (w). This demonstrates that the processes which control how far drainage basins grow laterally (in a direction parallel to the mountain front) are affected by the width of the topography (W).

The location of drainage outlets strongly influences the architecture of adjacent sedimentary deposits. The mean outlet spacing may be calculated from the spacing ratio, if the half-width of the fault block is known. The observed variability in fault block spacing ratios means that the mean outlet spacing cannot be precisely determined.

ACKNOWLEDGEMENTS

We thank Philip Allen, Michael Ellis and Doug Burbank for their very constructive reviews. Niels Hovius is

thanked for his thorough discussion of the ideas presented in the paper. Joanne Wilkin, Karen King and Neville Jones are thanked for their help during the early stages of this research.

REFERENCES

Adams, J. (1985) Large-scale tectonic geomorphology of the Southern Alps, New Zealand: summary. In: *Tectonic Geomorphology* (Ed. by M. Morisawa and J. T. Hack), pp. 105–128. Allen and Unwin, Boston.

Allen, P. A. & Hovius, N. (1998) Sediment supply from landslide-dominated catchments: implications for basin margin fans. *Basin Res.*, **10,** in press.

Appel, E., Rosler, W. & Corvinus, G. (1991) Magneto-stratigraphy of the Miocene-Pleistocene Surai Khola Siwaliks in West Nepal. *Geophys. J. Int.*, **105,** 191–198.

Bell, J. W. & Katzner, T. (1990) Timing of late Quaternary faulting in the 1954 Dixie valley earthquake area, central Nevada. *Geology*, **18,** 622–625.

Bryson, R. A. & Hare, F. K. (1981) *World Survey of Climatology Volume 11: Climates of North America*. Elsevier, New York.

Bull, W. B. (1964) Geomorphology of segmented alluvial fans in Western Fresno County, California. *US Geol. Surv. Prof. Pap.*, **352-B**, 89–128.

Bull, W. B. & McFadden, L. D. (1977) Tectonic geomorphology north and south of the Garlock fault, California. In: *Geomorphology in Arid Regions. Proceedings of the Eight Annual Geomorphology Symposium* (Ed. by D. O. Doehring). State University of New York at Binghampton, Binghampton, New York.

Corvinus, G. (1990) Litho- and biostratigraphy of the Siwalik succession in Surai Khola area, Nepal. In: *Proceedings of the Symposium on vistas in Indian Palaeobotany* (Ed. by K. P. Jain and R. S. Tiwari), *Palaeobotanist*, **38,** 293–297.

Crone, A. J. & Machette, M. (1984) Surface faulting associated with the Borah Peak earthquake, central Idaho. *Geology*, **12,** 644–667.

Denny, C. S. (1965) Alluvial fans of the Death Valley region, California and Nevada. *US Geol. Surv. Prof. Pap.*, **466**.

Densmore, A. L. Ellis, M. A. & Anderson, R. L. (1997) Numerical experiments on the evolution of mountainous topography. *J. geophys. Res.*, in press.

Ekstrom, G., Stein, R. S., Eaton, J. P. & Eberhart-Phillips, D. (1992) Seismicity and geometry of a 110-km-long blind thrust fault; 1. the 1985 Kettleman Hills. California, earthquake. *J. geophys. Res.*, **97B4,** 4843–4864.

Flint, S. S. & Bryant, I. D. (1993) The geological modelling of hydrocarbon reservoirs and outcrop analogues. *Spec. Pub. Int. Ass. Sediment.*, **15**.

Gardner, T. W. & Sevon, W. D. (1989) *Appalachian Geomorphology*. Elsevier, New York.

Hooke, R. LeB. & Rohrer, W. L. (1979) Geometry of alluvial fans: Effect of discharge and sediment size. *Earth surf. Process.*, **4,** 147–166.

Hovius, N. (1996) Regular spacing of drainage outlets from linear mountain belts. *Basin Res.*, **8,** 29–44.

Hovius, N. (1997) Macro scale process systems of mountain belt erosion. In: *Global Tectonics and Geomorphology* (Ed. by M. A. Summerfield). Wiley, New York, in press.

Howard, A. D. (1994) A detachment limited model of drainage basin evolution. *Water Resour. Res.*, **30,** 2261–2285.

Jackson, J. & Leeder, M. R. (1994) Drainage systems and the development of normal faults: an example from Pleasant Valley, Nevada. *J. struct. Geol.*, **16,** 1041–1059.

Jackson, J., Norris, R. & Youngson, J. (1996) The structural evolution of active fault and fold systems in central Otago. New Zealand: evidence revealed by drainage patterns *J. struct. Geol.*, **18,** 217–235.

Keller, E. A. & Pinter, N. (1996) *Active Tectonics: Earthquakes, Uplift, and Landscape*. Prentice Hall, New York, pp. 138–139.

Kostaschuk, R. A., Macdonald, G. M. & Putnam, P. E. (1986) Depositional process and alluvial fan-drainage basin morphometric relationships near Banff, Alberta, Canada. *Earth surf. Process. Landforms*, **11,** 471–484.

Kumar, R. (1993) Coalescence megafan: multistorey sandstone complex of the late orogenic (Mio-Pliocene) sub-Himalayan belt, Dehra Dun, India. *Sediment. Geol.*, **85,** 327–337.

Leeder, M. R. (1991) Denudation, vertical crustal movements, and sedimentary basin infill. *Geol. Rdsch.*, **80,** 441–458.

Leeder, M. R. & Gawthorpe, R. L. (1987) Sedimentary models for extensional tilt-block/half graben basins. *Geol. Soc. Lond. Spec. Publ.*, **28,** 139–152.

Leeder, M. R. & Jackson, J. A. (1993) The interaction between normal faulting and drainage in active extensional basins, with examples from the western United States and central Greece. *Basin Res.*, **5,** 79–102.

Mayer, L. (1986) Tectonic geomorphology of escarpment and mountain fronts. In: *Active Tectonics* (Ed. by R. E. Wallace), pp. 125–135. National Academy of Science, USA.

Milliman, J. D. & Syvitski, J. P. M. (1992) Geomorphic/tectonic control of sediment discharge to the oceans: The importance of small mountainous rivers. *J. Geol.*, **100,** 525–544.

Montgomery, D. R. & Dietrich, W. E. (1992) Channel initiation and the problem of landscape scale. *Science*, **255,** 826–830.

Morisawa, M. E. (1964) Development of drainage systems on an upraised lake floor. *Am. J. Sci.*, **262,** 340–354.

Mosley, M. P. (1972) *An experimental study of rill erosion.* MSc thesis, Colorado State University, Fort Collins, Colorado, USA.

Mueller, K. & Talling, P. J. (1996) Geomorphic evidence for tear faults accommodating lateral propogation of an active fault-bend fold, Wheeler Ridge, California. *J. struct. Geol.*, **19**, 397–411.

Okaya, D. A. & Thompson, G. A. (1985) Geometry of Cenozoic extensional faulting: Dixie valley, Nevada. *Tectonics*, **4,** 107–125.

Ori, G. G. (1993) Continental deposystems of the Quaternary of the Po Plain (northern Italy). *Sediment. Geol.*, **83,** 1–14.

Pieri, M. & Groppi, G. (1981) Subsurface geological structure of the Po Plain, Italy. *CRNR, P.F. Geodinamica*, **414**.

Ranga Rao, A. (1986) North-west Himalayan Foothills: Its stratigraphic record and tectonic phases. *Bull. Oil Natural Gas Commission*, **23-2,** 109–128.

Schumm, S. A. (1956) The evolution of drainage systems and slopes in badlands at Perth Amboy, New Jersey. *Bull. Geol. Soc. Am.*, **67,** 597–646.

Schumm, S. A., Mosley, M. P. & Weaver, W. E. (1987) *Experimental Fluvial Geomorphology*, pp. 29–32. Wiley-Interscience, New York.

Scott, W. E., Pierce, K. L. & Hait, M. H. (1985) Quaternary tectonic setting of the 1983 Borah Peak earthquake, central Idaho. *Bull. Seismol. Soc. Am.*, **75,** 1053–1066.

Sinha, R. S. & Friend, P. F. (1994) River systems and their sediment flux, Indo-Gangetic Plain, north Bihar, India. *Sedimentology*, **41,** 825–845.

Suppe, J. (1983) Geometry and kinematics of fault-bend folding. *Am. J. Sci.*, **283,** 684–721.

Takahashi, K. & Arakawa, H. (1981) *World Survey of Climatology Volume 9: Climates of southern and western Asia*. Elsevier, New York.

Talling, P. J., Hovius, N., Stewart, M. D., Kirkby, M. J., Gupta, S., Wilkin, J. C. & Stark, C. P. (1993) Regular spacing of drainage basin outlets: implications for basin fill architecture. *Abstract, British Sedimentological Research Group, Annual meeting, Manchester*.

Talling, P. J., Kirkby, M. J. & Leeder, M. R. (1992) Quantitative measurement of recent sediment mass transport in the Po drainage basin, northern Italy: a constraint upon modelling of alluvial basin fills. *Abstract, British Sedimentological Research Group, Annual meeting, Southampton*.

Walcott, R. I. (1978) Present tectonics and late Cenozoic evolution of New Zealand. *Geophys. J. Royal Astron. Soc.*, **52,** 137–164.

Wallace, R. E. (1978) Geometry and rates of changes of fault-generated range fronts, north-central Nevada. *US Geol. Surv. J. Res.*, **6,** 637–650.

Williams, R. B. G. (1984) *Introduction to Statistics for Geographers and Earth Scientists*. McMillan, London.

Woodring, W. P., Stewart, R. & Richards, R. W. (1940) Geology of the Kettleman Hills oil field, California. *US Geol. Surv. Prof. Pap.*, **195**.

Yamanaka, H. & Yagi, H. (1984) Geomorphological development of the Dang Dun, Sub-Himalayan zone, south-western Nepal. *J. Nepalese Geol. Soc.*, **4,** 151–159.

Yeats, R. S. & Lillie, R. J. (1991) Contemporary tectonics of the Himalayan frontal fault system: folds, blind thrusts and the 1905 Kangra earthquake. *J. struct. Geol.*, **13,** 215–225.

Zepeda, R. L., Keller, E. A., Rockwell, T. K. & Ku, T-L. (1998) Active tectonics and soil chronology of Wheeler Ridge, Southern San Joaquin Valley, California. *Geol. Soc. Am. Bull.*, in press.

Received 11 November 1996; revision accepted 11 August 1997

APPENDIX 1

Table 2 contains data measured from individual drainage basins.

APPENDIX 2

Mean outlet spacing (S) and mean topographic half-width (W) were measured a second time for the fault blocks used in this study (Table 3). A comparison of the measurements made in the two measurement runs allows the uncertainties involved in measuring spacing ratios to be addressed. For the second measurements, values of the mean topographic half-width (W) were calculated in a slightly different way. Topographic half-widths (w) were measured at selected localities, rather than at each drainage basin. Rigorous cut-off distances to determine which drainage outlets were to be included (i.e. 70% and 2% of the half-width) were not used in this second measurement run. Discrepancies in the spacing ratios measured only exceed 20% of the spacing ratio given in Table 1 if there was disagreement of the rivers included in the measurement procedure (Table 3). The differences in the spacing ratios, for locations where there were no changes in the number of outlets considered, is $\pm 20\%$ of the spacing ratio shown in Table 1. This comparison suggests that a very conservative estimate of the uncertainties involved in measuring the spacing ratio is $\pm 20\%$. The variability in spacing ratios seen on fault blocks cannot be explained as due to such an uncertainty, and is thus not due to measurement uncertainties (Fig. 7).

APPENDIX 3

A two-sample t-test (Williams, 1984, pp.169–173) was performed to quantitatively investigate whether the distribution of spacing ratios on different fault blocks was statistically different. Spacing ratio distributions from each location in Table 1 were compared with the distribution of spacing ratios from the fault block with the median spacing ratio (the north side of McGee Mountains). The test assumes that the sample distribution is drawn at random from a normally distributed parent population. Of the 42 comparisons made, 14 showed that at the 90% probability level the distributions came from populations with different means and variances (Table 3). Distributions of spacing ratios from mountain belts (Hovius, 1996) were similarly compared to the distribution of spacing ratios from the mountain belt with the median spacing ratio (Apennines). At the 90% probability level there was no difference between the distribution of spacing ratios from any of these mountain belts (Table 3). This shows that spacing ratios from different fault blocks are much more likely to be statistically different than the spacing ratios of the mountain belts studied by Hovius (1996).

Table 2. Data used to calculate mean fault-block spacing ratios (R) in Table 1.

Location	Outlet spacing (s in km)	Half-width (w in km)	Relief (h in m)	Gradient	Individual basins spacing ratio
Tilt Blocks					
Tobin Range	1.00	3.75	604.2	161	1.55
(1)	1.50	3.50	483.4	138	1.08
	1.50	3.25	604.2	186	0.800
	2.00	2.75	513.6	187	4.67
	0.700	2.75	574.0	209	4.00
	0.750	2.50	785.5	314	3.40
	1.75	2.75	828.7	301	3.00
	0.750	3.25	785.5	242	3.50
	1.00	3.25	1027	316	1.60
	1.00	3.00	1140	380	1.33
mean values	1.20	3.08	735.0	239	2.49
Stillwater Range	2.50	2.75	923.0	336	1.22
Dixie Valley	1.00	3.25	936.6	288	4.33
(2)	2.00	3.75	906.3	242	1.50
	0.750	2.50	906.3	363	1.25
	1.25	5.00	845.9	169	2.22
	2.50	5.50	968.6	176	1.83
	2.00	4.25	987.6	232	3.40
	2.50	3.75	1148	306	1.67
	1.25	3.25	1269	390	1.86
	1.50	7.25	1269	175	2.64
	1.50	7.00	994.0	142	2.33
mean values	1.70	4.39	1014	231	2.20
Humboldt Range	1.00	5.25	1329	266	6.67
(west side)	1.75	5.50	1495	285	2.33
(3)	0.500	5.75	1511	275	2.20
	3.75	5.25	1511	302	2.86
	0.750	4.75	1521	338	0.818
	2.50	5.25	1208	242	2.00
	1.50	5.00	1269	267	1.27
	2.50	4.85	1269	276	1.84
	2.50	5.50	1233	235	1.75
	2.25	5.50	1233	235	1.91
	1.00	5.25	1244	249	2.00
	2.00	5.75	1118	203	3.14
	3.00	5.25	621.8	124	1.54
mean values	1.92	5.30	1274	252	2.33
Humboldt Range	4.00	5.75	1611	280	1.44
(east side)	4.00	6.50	1586	244	1.62
(4)	5.00	7.75	1541	199	1.55
	5.25	6.25	1309	209	1.19
	4.75	7.00	1335	191	1.47
	5.25	6.75	712.4	106	1.29
mean values	4.71	6.62	1349	204	1.43
Clan Alpine Range	2.25	5.25	997.0	190	2.33
(east side)	1.50	5.50	1027	187	3.67
(5)	2.25	5.25	1118	213	2.33
	1.00	6.25	1011	162	6.25
	2.00	4.50	664.7	148	2.25
	1.00	5.25	845.9	161	5.25
	4.00	5.75	906.3	158	1.44
	4.50	7.00	725.1	90.6	3.20
	2.50	8.00	725.1	104	1.56

Table 2. (*continued*).

Location	Outlet spacing (s in km)	Half-width (w in km)	Relief (h in m)	Gradient	Individual basins spacing ratio
	1.25	6.00	1077	180	4.80
	2.50	6.00	966.8	161	2.40
mean value	2.25	5.89	915.0	155	3.23
Clan Alpine Range	3.75	6.75	1269	195	2.89
(west side)	2.50	6.00	1390	242	2.87
(6)	1.25	6.00	1269	221	5.75
	1.00	6.75	1283	197	4.33
	2.00	5.25	1057	211	1.67
	2.50	7.00	1027	152	1.69
mean values	2.16	6.29	1216	201	3.50
Stillwater Range	3.00	4.50	906.3	201	1.20
(west side)	3.00	3.25	1027	316	1.08
(7)	1.25	2.00	1027	514	1.33
	2.00	3.00	953.2	318	1.33
	3.00	3.50	906.3	259	1.08
	2.00	3.50	906.3	259	2.00
	2.50	3.00	845.9	282	1.09
	1.50	3.50	906.3	259	3.50
	2.50	3.75	1118	298	0.882
	3.75	5.00	1088	218	2.50
	1.25	5.00	1148	230	3.33
	1.50	5.50	1242	226	3.14
mean values	2.27	3.79	1006	265	1.87
Stillwater Range	2.25	6.50	1174	181	2.89
(northeast side)	3.25	6.75	1027	152	2.08
(8)	1.50	7.00	1148	164	4.67
	0.750	4.75	1148	242	6.33
	1.75	4.50	1088	242	2.57
mean values	1.90	5.90	1117	189	3.71
Sheep Range	2.25	4.50	1148	255	2.00
(9)	2.50	4.25	1148	270	1.70
	2.50	4.50	966.8	215	1.80
	1.75	3.50	1088	311	2.00
	1.75	3.25	966.8	297	1.86
	3.50	4.00	966.8	242	1.14
	1.75	3.25	1027	316	1.86
	2.50	4.50	845.9	188	1.80
	3.50	4.50	1148	255	1.29
mean values	2.44	4.03	1034	257	1.72
Toiyabe Range	2.50	4.00	664.7	166	1.78
(east side)	1.25	3.25	1148	353	3.25
(10)	1.50	3.50	1148	328	2.33
	1.75	3.50	1027	293	1.75
	1.25	4.50	1239	275	3.60
	1.50	4.50	1269	282	3.60
	1.50	3.75	1178	314	1.87
	2.25	3.75	1260	336	2.14
	0.250	3.75	1390	371	2.14
mean values	1.53	3.83	1147	299	2.50
Toiyabe Range	2.50	7.00	966.8	138	2.80
(west side)	0.750	7.00	1148	164	9.33
(11)	5.25	8.75	1232	141	1.59

Table 2. (*continued*).

Location	Outlet spacing (s in km)	Half-width (w in km)	Relief (h in m)	Gradient	Individual basins spacing ratio
	1.50	8.25	1196	145	8.25
	7.25	8.00	966.8	121	10.7
	8.50	8.25	997.0	121	1.18
mean values	4.29	7.87	1084	138	5.64
Panamint Range	2.75	12.5	1994	160	4.55
(southwest side)	3.75	12.2	2296	187	2.88
(12)	6.00	11.5	2613	227	2.09
	3.00	11.5	2186	190	2.71
	3.25	11.7	1692	144	2.94
	1.75	9.75	1773	182	3.55
mean values	3.42	11.5	2092	181	3.12
Panamint Range	5.00	8.50	2115	249	1.70
(southeast side)	4.50	11.7	2417	206	2.47
(13)	6.50	12.0	2734	228	2.18
	2.25	12.0	2307	192	1.66
	5.00	11.0	2498	227	3.38
mean values	4.65	11.1	2414	218	2.26
White Mountains	6.00	6.00	1934	322	0.550
(west side)	2.25	6.00	2115	352	0.667
(14)	1.75	5.50	2259	411	2.00
	1.50	5.50	2054	374	2.38
	2.00	5.75	2054	357	1.19
	2.25	5.75	2160	376	2.40
	3.00	7.50	2236	298	2.34
	2.00	8.50	2175	256	9.62
	2.00	7.25	2356	325	3.30
	2.25	8.00	2477	310	3.65
	3.25	9.00	2296	255	3.65
	1.75	9.75	2296	235	4.25
	2.50	8.25	2387	289	2.50
	3.25	8.50	2054	242	3.75
	4.00	8.50	2266	267	2.34
	3.50	8.75	2115	242	2.27
	4.00	10.5	2236	213	1.13
	2.00	10.7	2175	202	1.28
	2.50	8.75	2115	242	2.69
mean values	2.72	7.82	2198	281	2.73
White Mountain	2.50	11.7	1873	159	2.11
(east side)	5.25	11.0	2296	209	2.00
(15)	7.00	10.5	2356	224	1.07
	5.50	12.0	2296	191	2.15
	3.25	13.7	2795	203	1.29
mean values	4.70	11.8	2323	197	1.72
Sagre Del Cristo	1.25	7.00	1480	211	5.60
Mou	2.75	7.50	1571	209	2.73
(further north)	4.50	7.75	1631	211	1.72
(16)	2.25	6.75	1571	233	3.00
	4.25	6.75	1390	206	1.59
mean values	3.00	7.00	1529	218	2.93
Sagre Del cristo	1.75	5.00	1360	272	2.86
(further south)	0.500	5.00	1208	242	10.0
(17)	0.500	5.00	1208	242	10.0

Table 2. (*continued*).

Location	Outlet spacing (s in km)	Half-width (w in km)	Relief (h in m)	Gradient	Individual basins spacing ratio
	3.75	5.25	1208	230	1.30
	0.750	5.25	966.8	184	7.00
	1.00	4.25	1088	256	4.25
	4.00	3.50	1088	311	0.875
	1.75	3.25	1088	335	1.80
	0.500	3.75	664.7	177	7.50
	2.00	3.25	543.8	167	1.62
	2.00	3.50	785.5	224	1.75
	0.500	4.00	785.5	196	8.00
	1.00	4.00	966.8	242	4.00
	1.75	4.75	664.7	140	2.71
mean values	1.55	4.26	973.2	230	4.55
Pahsimeroi	0.500	3.25	664.7	205	6.50
Mountains	0.500	2.50	664.7	266	5.00
(18)	1.25	2.25	664.7	295	1.80
	1.00	2.50	634.4	254	2.50
	0.500	2.50	694.9	278	5.00
	0.750	2.50	664.7	266	3.33
	1.25	2.50	694.9	278	2.00
	2.75	3.00	664.7	222	1.09
	0.750	3.00	634.4	211	4.00
	1.25	3.00	664.7	222	2.40
mean values	1.05	2.70	665.0	246	3.36
Lemhi Range	4.25	5.75	1148	200	1.35
(west side)	1.25	5.00	1208	242	4.00
(19)	4.25	5.25	1057	201	1.24
	3.25	5.25	1088	207	1.62
	1.50	5.00	1088	218	3.33
	3.50	5.75	1088	189	1.64
	2.75	5.50	1148	209	2.00
mean values	2.96	5.36	1118	209	2.17
Lemhi Range	2.75	9.00	845.9	94.0	3.27
(east side)	5.75	6.00	845.9	141	1.04
(20)	3.00	4.75	755.3	159	1.58
	1.75	4.50	906.3	201	2.57
	4.75	4.00	785.5	196	0.842
	1.00	4.25	906.3	213	4.25
	3.50	4.50	845.9	188	1.29
	0.500	5.00	1027	205	10.0
	0.500	5.00	725.1	145	10.0
	6.00	5.75	1027	179	0.958
	4.25	5.50	966.8	176	1.29
	5.25	5.50	785.5	143	1.05
	0.500	5.50	785.5	143	11.0
	0.750	5.50	845.9	154	7.33
mean values	2.88	5.34	861.0	161	4.03
Growth Folds					
Kettleman Hills	0.444	1.96	63.44	32.3	4.43
Middle dome	1.14	2.28	81.57	35.8	2.00
(west side)	0.444	2.38	69.49	29.2	5.36
(21)	0.507	2.38	69.49	29.2	4.69
	0.919	2.28	63.44	27.8	2.48
	0.887	2.47	57.40	23.2	2.79
	0.412	2.15	51.36	23.8	5.23

Table 2. (*continued*).

Location	Outlet spacing (s in km)	Half-width (w in km)	Relief (h in m)	Gradient	Individual basins spacing ratio
	0.570	2.38	54.38	22.9	4.17
mean values	0.670	2.29	64.00	27.9	3.89
Kettleman Hills	0.824	1.55	114.8	73.9	1.88
Middle dome	0.475	1.74	114.8	65.9	3.67
(west side bend)	0.127	1.65	90.63	55.0	13.0
(22)	0.951	1.96	102.7	52.3	2.07
	0.475	2.22	108.8	49.0	4.67
	1.01	2.41	90.63	37.6	2.38
	1.14	2.25	69.49	30.9	1.97
	1.30	2.12	51.36	24.2	1.63
mean values	0.790	1.99	93.00	46.7	3.91
Kettleman Hills	0.729	3.17	43.81	13.8	4.35
North Dome	1.30	2.72	37.76	13.9	2.10
(west side)	0.380	3.04	60.42	19.9	8.00
(23)	1.27	3.23	83.08	25.7	2.55
	2.44	3.55	74.02	20.9	1.45
	1.93	3.30	75.53	22.9	1.70
	1.01	3.26	105.7	32.4	3.22
mean values	1.29	3.18	68.60	21.6	3.34
Kettleman Hills	0.634	2.06	105.7	51.3	3.25
North Dome	0.634	1.74	105.7	60.7	2.75
(far north side)	0.222	2.03	105.7	52.1	9.14
(24)	0.602	1.90	93.05	48.9	3.16
	0.190	1.81	103.6	57.4	9.50
	0.158	2.09	70.09	33.5	13.2
	0.729	2.06	107.6	52.2	2.83
	1.01	2.06	105.7	51.3	2.03
	0.824	1.96	111.2	56.6	2.38
mean values	0.560	1.97	101.0	51.3	5.36
North Dome	2.82	4.18	157.1	37.6	1.48
(east side)	2.28	4.50	158.6	35.3	1.97
(25)	0.634	4.44	166.2	37.5	7.00
	2.82	4.56	166.2	36.4	1.62
	5.20	4.56	151.1	33.1	0.878
mean values	2.75	4.45	160.0	36.0	2.59
Dundwa Range	2.50	7.25	600.9	82.9	2.90
(North Side)	3.25	6.75	604.2	89.5	2.08
(26)	2.00	5.75	604.2	105	2.87
	1.50	5.75	710.0	123	3.83
	1.37	5.50	619.3	113	4.00
	1.75	5.50	619.3	113	3.14
	1.37	6.50	574.0	88.3	4.73
	2.37	7.00	604.2	86.3	2.95
	2.87	6.50	679.8	105	2.26
	3.00	8.00	755.3	94.4	2.67
mean values	2.20	6.45	612.0	94.9	3.14
Dundwa Range	0.858	4.72	755.3	160	5.50
(South side)	3.00	4.72	755.3	160	1.57
(27)	2.15	4.72	755.3	160	2.20
	1.72	4.72	710.0	150	2.75
	1.29	5.58	619.3	111	4.33
	0.858	5.58	634.4	114	6.50

Table 2. (*continued*).

Location	Outlet spacing (s in km)	Half-width (w in km)	Relief (h in m)	Gradient	Individual basins spacing ratio
	4.29	5.15	604.2	117	1.20
	1.29	4.72	679.8	144	3.67
	3.00	5.15	755.3	147	1.71
	2.15	6.01	830.8	138	2.80
	3.00	6.87	755.3	110	2.29
	4.29	6.87	856.5	125	1.60
	1.72	6.87	830.8	121	4.00
	3.86	6.87	755.3	110	1.78
	5.15	6.44	604.2	93.9	1.25
	3.43	6.44	679.8	106	1.87
	4.29	6.44	679.8	106	1.50
mean values	2.72	5.76	721.3	125	2.74
West of Girwa River	1.50	5.75	1148	200	3.83
(28)	2.00	5.75	1163	202	2.87
	1.25	5.50	1163	211	4.40
	0.625	5.50	1148	209	8.80
	1.12	5.75	1163	202	5.11
	1.87	5.87	1208	206	3.13
	1.12	5.75	1179	205	5.11
	1.62	5.50	1208	220	3.38
	1.37	6.00	1210	202	4.36
	1.25	5.87	1239	211	4.70
	1.50	5.75	1241	216	3.83
	1.62	5.87	1208	206	3.62
	0.750	5.37	1057	197	7.17
	1.50	5.50	1163	211	3.67
	0.750	5.75	1200	209	7.67
	0.500	5.37	1178	219	10.7
	2.00	5.62	1148	204	2.81
	2.62	5.25	1178	224	2.00
mean values	1.39	5.65	1178	208	4.84
Churia Range	0.750	4.62	755.3	163	6.17
S. of Babai R.	7.37	4.62	604.2	131	0.627
(29)	2.00	5.00	700.9	140	2.50
	1.25	4.62	604.2	131	3.70
	1.37	4.75	604.2	127	3.45
	3.00	4.00	771.0	193	1.33
	1.37	3.62	771.0	213	2.64
	2.00	4.50	604.2	134	2.25
	1.50	4.62	604.2	131	3.08
	1.75	3.50	755.3	216	2.00
	1.00	3.37	488.8	145	3.37
	1.25	3.75	604.2	161	3.00
	1.25	3.50	604.2	173	2.80
	1.12	3.25	604.2	186	2.89
	3.00	4.75	781.3	164	1.58
	1.75	5.00	755.3	151	2.86
	1.75	5.25	755.3	144	3.00
	4.00	4.12	755.3	183	1.03
	3.37	4.12	604.2	146	1.22
	2.50	3.75	860.4	229	1.50
	1.62	3.62	860.4	237	2.23
	0.750	3.25	891.2	274	4.33
	1.50	3.00	755.3	252	2.00
	1.50	3.00	755.3	252	2.00
	0.625	2.75	828.7	301	4.40

Table 2. (*continued*).

Location	Outlet spacing (s in km)	Half-width (w in km)	Relief (h in m)	Gradient	Individual basins spacing ratio
	1.62	3.00	755.3	252	1.85
	1.37	3.37	604.2	179	2.45
	0.375	3.00	604.2	201	8.00
	2.25	3.25	755.3	232	1.44
	0.625	3.25	828.1	255	5.20
	1.75	3.25	828.1	255	1.86
	1.75	3.25	679.8	209	1.86
	2.37	3.25	755.3	232	1.37
	1.37	3.50	755.3	216	2.55
	1.00	3.75	755.3	201	3.75
	1.62	3.75	755.3	201	2.31
	1.12	3.75	755.3	201	3.33
	1.00	4.00	942.9	236	4.00
	0.750	3.62	942.6	260	4.83
	1.00	3.37	755.3	224	3.37
	1.00	3.50	755.3	216	3.50
	2.25	3.87	830.8	214	1.72
	2.12	3.12	841.1	269	1.47
mean values	1.74	3.77	734.0	195	2.81
Churia Range	1.50	1.87	1012	540	0.750
No. of Babai River	0.750	2.50	1057	423	2.50
(30)	1.00	2.62	1057	403	3.00
	0.750	2.62	1142	435	2.10
	1.00	2.87	1142	397	2.30
	1.25	2.75	1057	385	2.44
	1.00	2.50	1057	423	2.00
	1.25	3.50	1057	302	2.80
	0.750	3.62	1057	292	5.80
	0.500	3.50	1057	302	4.52
	0.750	3.50	1133	324	1.47
	2.25	3.75	1208	322	1.67
	1.25	4.37	1273	291	0.833
	1.00	3.00	1057	352	4.00
	1.25	3.00	1188	396	3.00
	0.750	4.50	981.9	218	1.89
	1.25	4.50	981.9	218	1.89
	1.50	5.00	1050	210	2.00
	0.750	4.75	1057	223	6.33
	1.00	4.87	1133	232	3.25
	2.50	5.62	1133	201	3.21
	2.50	5.25	1134	216	1.62
	2.50	4.62	1133	245	1.95
	1.50	4.25	1133	267	1.70
	1.00	5.00	1057	211	2.86
	1.75	4.50	906.3	201	1.80
	3.25	3.25	906.3	279	1.53
	2.25	3.50	968.9	277	1.00
	2.50	3.50	993.4	284	2.80
	2.25	3.25	1106	340	1.04
	2.75	3.50	1057	302	28.0
	2.25	3.75	1057	282	2.00
	3.50	4.00	1057	264	1.33
	1.25	4.12	1136	275	2.06
	3.25	3.25	906.3	279	1.62
	1.75	3.25	906.3	279	2.60
	3.00	3.12	906.3	290	2.08
	2.00	2.75	906.3	330	5.50
mean values	1.66	3.69	1057	286	2.51

Table 2. (*continued*).

Location	Outlet spacing (s in km)	Half-width (w in km)	Relief (h in m)	Gradient	Individual basins spacing ratio
Chandigarh Dun	2.50	7.10	210.0	29.6	2.84
(31)	2.60	7.82	200.0	25.6	3.01
	2.30	8.16	190.0	23.3	3.55
	1.60	8.50	190.0	22.4	5.31
	1.60	8.50	240.0	28.2	5.31
	3.60	7.82	230.0	29.4	2.17
	0.640	8.12	210.0	25.9	12.7
	3.32	8.14	240.0	29.5	2.45
	3.00	9.10	220.0	24.2	3.03
	3.00	7.60	170.0	22.4	2.53
	2.00	7.60	210.0	27.6	3.80
	3.60	6.64	210.0	31.6	1.84
mean values	2.48	7.93	210.0	26.5	4.05
Old Topography					
River Mountains	0.240	0.432	120.8	280	1.80
(south side)	0.0720	0.432	132.9	308	6.00
(32)	0.360	0.480	120.8	252	1.33
	0.120	0.528	120.8	229	4.40
	0.300	0.516	120.8	234	1.72
	0.348	0.576	108.8	189	1.66
	1.01	0.540	108.8	201	0.536
	0.192	0.612	151.1	247	3.19
	0.120	0.540	120.8	224	4.50
	0.660	0.600	151.1	252	0.909
	0.144	0.528	117.8	223	3.67
	0.528	0.540	114.8	213	1.02
mean values	0.340	0.530	124.0	234	2.56
Goshen Mountains	0.192	0.480	211.5	441	3.38
(north side)	0.120	0.504	211.5	420	5.70
(33)	0.168	0.480	169.2	352	4.07
	0.0360	0.504	163.1	324	19.0
	0.156	0.504	145.0	288	4.31
	0.288	0.504	157.1	312	2.54
	0.288	0.528	157.1	297	2.50
	0.192	0.504	157.1	312	3.50
	0.156	0.504	157.1	312	4.15
	0.156	0.504	139.0	276	4.15
	0.276	0.504	187.3	372	2.13
	0.360	0.528	187.3	355	1.57
	0.216	0.528	181.3	343	2.61
	0.168	0.528	169.2	320	3.57
	0.108	0.528	187.3	355	4.83
	0.192	0.552	187.3	339	2.50
	0.180	0.552	175.2	317	2.73
	0.336	0.552	181.3	328	1.50
	0.336	0.552	175.2	317	1.50
mean values	0.210	0.520	174.0	335	2.90
Goshen Mountains					
(south side)	0.384	0.480	211.5	441	1.25
(34)	0.432	0.408	151.1	370	0.944
	0.216	0.284	157.1	409	1.78
	0.288	0.408	157.1	385	1.42
	0.0960	0.396	151.1	381	4.13

Table 2. (*continued*).

Location	Outlet spacing (s in km)	Half-width (w in km)	Relief (h in m)	Gradient	Individual basins spacing ratio
	0.192	0.360	139.0	386	1.88
	0.0480	0.360	139.0	386	7.50
	0.108	0.348	139.0	399	3.22
	0.168	0.336	139.0	414	2.00
	0.0720	0.348	139.0	399	4.83
	0.144	0.384	157.1	409	2.67
	0.168	0.372	151.1	406	2.21
	0.0600	0.372	139.0	374	6.20
	0.132	0.384	145.0	378	2.91
	0.144	0.384	151.1	393	2.67
	0.192	0.360	157.1	436	1.88
	0.192	0.360	157.1	436	1.88
	0.0360	0.336	139.0	414	9.33
	0.228	0.336	139.0	414	1.47
	0.0600	0.336	157.1	467	5.60
	0.324	0.324	157.1	485	1.00
mean values	0.180	0.370	151.0	408	3.18
North McGee Mtn	0.192	0.960	157.1	164	5.00
(35)	0.840	0.888	163.1	184	1.06
	0.672	0.912	151.1	166	1.36
	0.552	0.840	163.1	194	1.52
	0.792	0.816	169.2	207	1.03
mean values	0.610	0.880	161.0	183	1.99
McGee Mountains	0.240	0.528	214.5	406	2.20
(north side)	0.336	0.528	208.5	395	1.57
(36)	0.360	0.528	208.5	395	1.47
	0.240	0.504	199.4	396	2.10
	0.0960	0.456	208.5	457	4.75
	0.144	0.480	208.5	434	3.33
	0.144	0.456	208.5	457	3.17
	0.0960	0.456	184.3	404	4.75
	0.216	0.432	202.4	468	2.00
	0.240	0.456	208.5	457	1.90
	0.216	0.480	208.5	434	2.22
	0.144	0.504	211.5	420	3.50
	0.144	0.504	217.5	432	3.50
	0.168	0.504	217.5	432	3.00
	0.216	0.528	223.6	423	2.44
mean value	0.200	0.490	209.0	427	2.79
McGee Mountains	0.240	0.672	169.2	252	2.80
(south side)	0.360	0.648	181.3	280	1.80
(37)	0.192	0.624	175.2	281	3.25
	0.288	0.600	175.2	292	2.08
	0.288	0.576	169.2	294	2.00
	0.192	0.552	175.2	317	2.88
	0.240	0.528	175.2	332	2.20
	0.312	0.504	175.2	348	1.62
	0.312	0.456	151.1	331	1.46
	0.0960	0.456	169.2	371	4.75
	0.312	0.432	175.2	406	1.38
	0.216	0.432	181.3	420	2.00
	0.288	0.456	190.3	417	1.58
mean value	0.260	0.530	174.0	328	2.29

Table 2. (*continued*).

Location	Outlet spacing (s in km)	Half-width (w in km)	Relief (h in m)	Gradient	Individual basins spacing ratio
Bays Mountain	1.78	1.02	241.7	237	0.574
(north side)	0.312	1.19	287.0	242	3.81
(38)	1.28	1.15	253.8	220	0.897
	0.336	1.19	284.0	239	3.54
	1.09	1.08	284.0	263	0.989
mean values	0.960	1.13	270.0	239	1.96
Bays Mountain	0.0720	1.03	259.8	252	14.3
(south side)	0.312	0.960	253.8	264	3.08
(39)	0.312	0.984	250.8	255	3.15
	0.228	0.912	271.9	298	4.00
	0.216	0.828	271.9	328	3.83
	0.276	0.840	271.9	324	3.04
	0.468	0.852	241.7	284	1.82
	0.216	0.900	253.8	282	4.17
	0.264	0.888	271.9	306	3.36
	0.0960	0.864	265.9	308	9.00
	0.312	0.840	259.8	309	2.69
	0.168	0.768	235.6	307	4.57
	0.180	0.720	277.9	386	4.00
	0.300	0.864	271.9	315	2.88
	0.336	0.888	265.9	299	2.64
mean values	0.250	0.880	262.0	298	4.44
Non-Linear					
Shoshone range	6.00	8.50	1414	166	1.42
(40)	4.25	5.75	1414	246	1.35
	4.00	5.25	1118	213	1.31
	2.00	5.00	725.1	145	2.50
	1.75	7.50	634.4	84.6	4.29
	5.00	10.0	818.7	81.9	2.00
	3.25	6.75	815.7	121	2.08
	5.00	4.25	302.1	71.1	0.850
	8.75	7.25	574.0	79.2	0.829
	3.00	5.50	973.1	177	1.83
	2.00	5.75	800.6	139	2.87
	2.75	5.00	694.9	139	1.82
	4.50	5.50	754.5	137	1.22
mean value	4.02	6.31	849.0	135	1.87
Sonoma Range	5.00	6.00	1088	181	1.05
(41)	11.2	8.25	1269	154	0.489
	3.55	9.75	1329	136	1.48
	5.25	8.00	935.0	117	0.810
	3.75	7.50	617.2	82.3	1.80
	2.25	5.25	453.2	86.3	2.22
mean values	5.18	7.46	949.0	127	1.31
Fox Range	1.25	3.50	365.0	104	2.80
(42)	1.25	5.75	423.0	73.6	4.60
	3.00	4.50	543.8	121	1.50
	4.50	4.25	665.9	157	0.944
	2.00	4.00	786.7	197	2.00
	1.25	4.00	785.5	196	3.20
	1.25	4.50	785.5	175	3.60
	3.00	7.00	908.8	130	2.33
	11.0	6.75	664.7	98.5	0.614
	10.7	7.50	518.4	69.1	0.698
mean values	3.93	5.18	645.0	125	2.23

Table 2. (*continued*).

Location	Outlet spacing (s in km)	Half-width (w in km)	Relief (h in m)	Gradient	Individual basins spacing ratio
East range	5.50	4.50	523.6	116	0.818
(43)	4.00	3.75	392.7	105	0.938
	2.00	3.50	332.3	95.0	1.75
	3.25	3.25	513.6	158	1.00
	2.50	4.00	513.6	128	1.60
	7.00	7.00	515.1	73.6	1.00
	6.50	8.25	574.0	69.6	1.27
	4.25	6.75	755.3	112	1.59
	10.7	5.50	838.7	152	0.512
	5.50	5.00	570.1	114	0.909
	2.00	7.00	604.2	86.3	3.50
	1.50	6.00	674.9	112	4.00
mean value	4.56	5.38	567.0	105	1.57

Table 3. Distribution of spacing ratios across a range of tilted fault blocks, growth folds and mountain belts.

Location no.	Name	Name	Spacing ratio (R)	Outlet spacing (S in km)	Half-width (W in km)	Spacing ratio (percentage change from R in Table 1)	Comment	t	P
Tilt Blocks									
	Nevada								
1	Tobin Range	East Side	2.66	1.31	3.49	−3.91		0.77509	>.20
2	Stillwater Range	Dixie Valley	2.82	1.45	4.09	−9.30		1.7982	<.20
3	Humboldt Range	West Side	3.32	1.77	5.87	−18.1		1.1810	>.20
4	Humboldt Range	East Side	1.30	4.68	6.10	7.80		3.0097	<.01
5	Clan Alpine Range	East Side	2.95	1.95	5.75	−12.6		0.85531	>.20
6	Clan Alpine Range	West Side	3.39	2.00	6.77	−16.5		4.3558	<.001
7	Stillwater Range	West Side	2.27	2.27	3.40	−35.9	new river	2.5104	<.05
8	Stillwater Range	Northeast Side	3.52	2.20	7.75	−13.2		1.4791	<.20
9	Sheep Range	(near Las Vegas)	1.79	2.47	4.42	−8.48		2.8478	<.01
10	Toiyabe Range	East Side	2.88	1.44	4.15	−15.2	new river	0.82282	>.20
11	Toiyabe Range	West Side	2.19	3.29	7.21	−20.3	new river	3.2128	<.02
	California								
12	Panamint Range	Southwest Side	3.44	3.54	12.2	−2.08		0.57409	>.20
13	Panamint Range	Southeast Side	2.41	4.65	11.2	−1.26		1.0728	>.20
14	White Mountain	West Side	3.18	2.66	8.45	−10.4		0.22814	>.20
15	White Mountain	East Side	2.85	4.33	12.3	−13.5		2.1702	<.05
	Colorado								
16	Sangre Del Cristo Mt	West Side	2.38	3.31	11.0	−2.15		0.15748	>.20
17	Sangre Del Cristo Mt	Southwest Side	3.34	7.62	18.1	−16.0		2.6046	<.10
	Idaho								
18	Pahsimeroi Mtns	West Side	2.23	2.65	5.92	13.2		0.16601	>.20
19	Lemhi Range	West Side	2.01	2.65	5.36	−11.0		1.4064	<.20
20	Lemhi Range	East Side	1.95	3.22	6.29	−5.41		1.5780	>.20
Growth Folds									
	California								
21	Kettleman Hills	Mid dome-west side	3.43	0.656	2.25	−0.292		2.2445	<.05
22	Kettleman Hills	Mid dome-west bend	2.88	0.660	1.90	−14.3		1.3595	>.20
23	Kettleman Hills	N. dome-west side	3.11	0.966	3.00	−25.9	new river	0.84964	>.20
24	Kettleman Hills	N. dome-farnorth sd	3.46	0.575	1.98	1.70		3.0556	<.05
25	Kettleman Hills	N. dome-NE side	1.21	2.87	3.48	25.3	new river	0.37245	>.20
	Nepal								
26	Dundwa Range	North Side	2.99	2.87	8.57	−2.05		0.76764	>.20
27	Dundwa Range	South Side	2.20	2.72	6.00	−3.77		0.24861	>.20
28	Range west of the	Girwa River	3.95	1.32	5.21	2.71		4.0010	<.01
29	Churia Range	S. of Babai River	2.52	1.98	4.97	−16.1		0.083569	>.20
30	Churia Range	N. of Babai River	2.55	1.63	4.17	−14.9		0.37247	>.20
31	Chandigarh Dun	South Side	2.81	2.53	7.11	12.2		1.9299	<.20
Old Topography									
	Appalachians								
32	River Mountains	South Side	1.26	0.378	0.480	19.2		0.59747	>.20
33	Goshen Mountains	North Side	2.51	0.207	0.520	−1.21		1.5887	>.20
34	Goshen Mountains	South Side	2.35	0.162	0.380	−14.1		0.70055	>.20
35	North McGee Mountain	South Side	1.26	0.643	0.810	12.5		1.5281	<.20
36	McGee Mountains	North Side	2.39	0.210	0.500	2.45		0.11996	N/A
37	McGee Mountains	South Side	2.22	0.236	0.520	−8.82		1.4760	<.20
38	Bays Mountain	North Side	1.36	0.824	1.12	−15.3		1.5297	<.20
39	Bays Mountain	South Side	3.81	0.243	0.930	−8.24		2.4684	<.10
Nonlinear Mountain Front									
	Nevada								
40	Shoshone Range		1.36	4.93	7.50	13.4		2.6057	<.05
41	Sonoma Range		1.61	5.29	6.80	−11.8		3.1791	<.01
42	Fox Range		1.48	3.70	4.47	−13.0		1.3801	>.20
43	East Range		1.39	3.58	5.76	−17.8		3.2197	<.01
Mountain Ranges	Southern Alps							3.7121	>.20
	Finisterre Range							0.51079	>.20
	Maoke Range							0.042180	>.20
	Barisan Range							1.3306	<.20
	Central Range							1.0786	>.20
	Himalaya							1.2415	<.20
	Tien Shan							1.3710	<.20
	Kirgizskiy Khrebet							0.43329	>.20
	Apennines							0.0000	N/A
	Sierra Nevada							0.75648	>.20
	Andes							0.18895	>.20

